Supplementary Appendix

This appendix has been provided by the authors to give readers additional information about their work.

Supplement to: Martínez VP, Di Paola N, Alonso DO, et al. “Super-spreaders” and person-to-person transmission of Andes virus in Argentina. N Engl J Med 2020;383:2230-41. DOI: 10.1056/NEJMoa2009040

Supplementary Appendix

"Super-Spreaders" and Person-to-Person Transmission of Andes Virus in Argentina

Valeria P. Martínez, PhD[1*], Nicholas Di Paola, ScD[2*], Daniel O. Alonso, BSc[1*], Unai Pérez-Sautu, PhD[2*], Carla M. Bellomo, PhD[1], Ayelén A. Iglesias, BSc[1], Rocio M. Coelho[1], BSc[1], Beatriz López, BSc[3], Natalia Periolo, PhD[1], Peter A. Larson, PhD[2], Elyse R. Nagle, MSc[2], Joseph A. Chitty, BSc[2], Catherine B. Pratt, MSc[2,4], Jorge Díaz, PhD[5], Daniel Cisterna, PhD[3], Josefina Campos, BSc[3], Heema Sharma, MSc[8], Bonnie Dighero-Kemp, BSc[8], Emiliano Biondo, MD[5], Lorena Lewis, BSc[6], Constanza Anselmo, BSc[6], Camila P. Olivera, BSc[6], Fernanda Pontoriero, BSc[7], Enzo Lavarra, MD[6], Jens H. Kuhn, MD[8], Teresa Strella, MD[9], Alexis Edelstein[10], PhD, Miriam I. Burgos, MD[11], Mario Kaler, MD[11], Adolfo Rubinstein, PhD[11], Jeffrey R. Kugelman, PhD[2], Mariano Sanchez-Lockhart, PhD[2,12], Claudia Perandones, PhD[13,‡], Gustavo Palacios, PhD[2,‡]

[1]Laboratorio Nacional de Referencia de Hantavirus, Instituto Nacional de Enfermedades Infecciosas, Administración Nacional de Laboratorios e Institutos de Salud "*Dr. Carlos G. Malbran*", Ciudad Autónoma de Buenos Aires CP1281, Argentina
[2]Center for Genome Sciences, United States Army Medical Research Institute of Infectious Diseases, Fort Detrick, Frederick, Maryland 21702, USA
[3]Plataforma Genomica, Instituto Nacional de Enfermedades Infecciosas, Administración Nacional de Laboratorios e Institutos de Salud "*Dr. Carlos G. Malbrán*", Ciudad Autónoma de Buenos Aires CP1281, Argentina
[4]College of Public Health, University of Nebraska Medical Center, Omaha 68198, Nebraska, USA
[5]Área Programática Esquel, Ministerio de Salud de Chubut, Esquel, Chubut CP9200, Argentina
[6]Hospital Zonal de Esquel, Ministerio de Salud de Chubut, Esquel, Chubut CP9200, Argentina
[7]Hospital Zonal de Bariloche "*Dr. Ramón Carrillo*", Ministerio de Salud de Río Negro, San Carlos de Bariloche CP8400, Río Negro, Argentina
[8]Integrated Research Facility at Fort Detrick, National Institute of Allergy and Infectious Diseases, National Institutes of Health, Fort Detrick, Frederick, Maryland 21702, USA
[9]Ministerio de Salud de Chubut, Rawson, Chubut CP9103, Argentina
[10]Unidad Operativa de Control y Contención Biológica, Administración Nacional de Laboratorios e Institutos de Salud "*Dr. Carlos G. Malbrán*", Ciudad Autónoma de Buenos Aires CP1281, Argentina
[11]Secretaría de Gobierno de Salud, Ministerio de Salud y Desarrollo Social de la Nación Argentina, Ciudad Autónoma de Buenos Aires CP1281, Argentina
[12]Department of Pathology and Microbiology, University of Nebraska Medical Center, Omaha 68198, Nebraska, USA
[13]Administración Nacional de Laboratorios e Institutos de Salud "*Dr. Carlos G. Malbrán*", Ciudad Autónoma de Buenos Aires CP1281, Argentina

* These authors contributed equally to the study
‡ These authors codirected the study

Corresponding authors:

Gustavo Palacios, Center for Genome Sciences, United States Army Medical Research Institute of Infectious Diseases (USAMRIID), 1425 Porter Street, Fort Detrick, Frederick, Maryland 21702, USA (gustavo.f.palacios.civ@mail.mil); Valeria P. Martínez, Laboratorio Nacional de Referencia para Hantavirus, Instituto Nacional de Enfermedades Infecciosas (INEI) Administración Nacional de Laboratorio e Institutos de Salud (ANLIS) "Dr. C. G. Malbrán," Avenida Vélez Sarsfield 563, Ciudad Autónoma de Buenos Aires 1281, Argentina (pmartinez@anlis.gob.ar)

Table of Contents

Methods

1.1 Ethics statement

The procedures for sampling and analysis of hantavirus pulmonary syndrome-suspected cases were approved by the Ethics Committee from Instituto Nacional de Genética Médica from ANLIS. Written informed consent was obtained from all patients and volunteers before analysis. The enrollment process included patients with suspected hantavirus pulmonary syndrome from November 2018 to February 2019. Samples from suspected hantavirus pulmonary syndrome cases from Epuyén Province were submitted for diagnosis confirmation to the Hantavirus National Reference Laboratory (Laboratorio Nacional de Referencia para Hantavirus, Instituto Nacional de Enfermedades Infecciosas, ANLIS).

Samples were shipped to USAMRIID under material transfer agreement (MRMC control number: W81XWH-18-0469) approved on September 27, 2018. The de-identified human diagnostic surveillance samples analyzed in this project were also reviewed for the applicability of human subjects protection regulations under the project, "Genomic Characterization of South American Hantavirus and Other Viral Agents," United States Army Medical Research Institute of Infectious Diseases (USAMRIID), Office of Human Use and Ethics, Log Number FY17–10.

CP and GP designed the study. VPM, ND, DOA, UP-S, CMB, AAI, RMC, BL, NP, PAL, ERN, JAC, CBP, JD, DC, JC, HS, BD-K, EB, LL, CA, CPO, FP, EL, TS, AE, MIB, MK, and AR gathered the data. VPM, ND, DOA, UP-S, CMB, AAI, MS-L, CP, and GP analyzed the data. All the authors vouch for the accuracy and completeness of the data. VPM, ND, DOA, and UP-S vouch for the analysis. VPM, ND, DOA, UP-S, JK, MS-L, CP, and GP wrote the paper. VPM, ND, CP, and GP decided to publish the paper.

1.2 Hantavirus pulmonary syndrome case definition

A suspected hantavirus pulmonary syndrome case was defined as a patient who resides in an endemic region (or reports a recent travel history to an endemic region) and/or had contact during the previous 40 days with a recently laboratory-confirmed hantavirus pulmonary syndrome case, and presents with a persistent fever (>48 h), headache, myalgia, and/or gastrointestinal manifestations (e.g., abdominal pain, vomiting, and/or diarrhea).[1-3]

A laboratory-confirmed hantavirus pulmonary syndrome case was defined as a suspected case with above-threshold titers of ANDV-specific IgM and IgG or real-time RT-qPCR-detectable circulating ANDV RNA.[4,5]

A secondary case was defined as a confirmed case who was in close contact with a previous hantavirus pulmonary syndrome case at the time of fever onset of the primary case and who developed symptoms or sign up to 40 days after contact with the primary case.

1.3 Severity classifications of clinical data

Disease severity was first classified according to clinical presentation in four different grades (**Table S1**). Briefly, Grade I encompasses patients with prodromal symptoms without respiratory compromise; Grade II encompasses patients with mild to moderate respiratory compromise

without hemodynamic compromise; Grade III encompasses patients with severe respiratory insufficiency with hemodynamic compromise; Grade IV encompasses patients with severe respiratory insufficiency and hemodynamic compromise that is refractory to treatment and associated with fatal outcome.

1.4 Further details on sequencing methods and genetic data generation

Whole-blood samples from 28 (82% of 34) laboratory-confirmed cases from the Epuyén ANDV-caused hantavirus pulmonary syndrome outbreak were included in the genomic analysis. We also sequenced the ANDV strains responsible for the 1996 outbreak in El Bolsón (Epilink/96) and a 1997 case in Bariloche (NRC-2/97),[6] along with strains of four ANDV-caused hantavirus pulmonary syndrome patients from the same year and geographic area (**Table S2**) as those from the Epuyén ANDV-caused hantavirus pulmonary syndrome outbreak, but without known epidemiological connection to this recent outbreak.

RNA was extracted from 400 µl of whole blood in TRIzol LS reagent using the TRIzol™ Reagent and Phasemaker™ Tubes Complete System (ThermoFisher Scientific, Waltham, MA, USA) following the manufacturer's protocol. RNA sequencing libraries were prepared using the KAPA RNA HyperPrep kit (KAPA Biosystems, Wilmington, MA, USA) following the manufacturer's guidelines. Unique dual-index pairs were used for library indexing with xGen Dual Index UMI Adaptors (Integrated DNA Technologies, Skokie, IL, USA), which also served as a control against contamination. Following library preparation, the Illumina TruSeq RNA Exome enrichment reagents were used with a custom ANDV-specific biotinylated probe set (Twist Biosciences, San Francisco, CA, USA) in singleplex reactions following the manufacturer's recommendations. The probe set included 3,822 unique probes of 120-nt in length for enrichment of the libraries for ANDV-specific sequences. Pooled libraries were sequenced on the Illumina (San Diego, CA) MiSeq or NextSeq sequencing platforms (Illumina, San Diego, CA) using 2 x 151-bp paired-end sequencing.

Sequencing reads were cleaned using Trimmomatic v0.381 and Cutadapt2 to remove Illumina adaptors and low-quality bases, followed by Prinseq-lite v0.20.43 to remove duplicate reads.[7-9] Human genome and human transcriptome read removal was subsequently performed by aligning quality-trimmed reads to the human genome reference GRCh38 (Genbank assembly accession: GCF_000001405.39) using Bowtie 2.4.[10]

To generate ANDV consensus genomes, cleaned reads were assembled de novo using SPAdes v3.9.0.5.[11] Gaps and ends of incomplete contigs were filled in with sequences from close complete genomic segments from GenBank (Chile-9717869 strain[12]: RefSeq accession numbers NC_003466.1, NC_003467.2, and NC_003468.2). We then used a *de novo* assembled ANDV-genome from this work as a reference to align clean reads with Bowtie 2.4. Duplicates were subsequently removed with Picard (Broad Institute, Cambridge, MA, USA), and a new consensus sequence was generated using a combination of SAMtools v0.1.186[13] and custom scripts.[14]

Only bases with a Phred quality score >Q20 and a minimum of 3X coverage were used for consensus calling. Consensus genome sequences from other ANDV cases were aligned using MAFFT v.7.397.[15] Geneious v7.1.3[16] was used to manually identify intra-outbreak ANDV single nucleotide polymorphisms (SNPs). Viral population diversity analysis was performed from the

sequencing data with a validated analysis pipeline (VSALIGN) as described previously.[17] For this purpose, we used the ANDV complete genome of Patient 1 as a reference of the ANDV consensus genome sequence of the outbreak. Default parameters in VSALIGN were used to determine the frequency of SNPs for every nucleotide position along the genome with a minimum depth of 100 reads.[18] The diversity of the viral population was then estimated according to two parameters: 1) the average frequency of SNPs in each genomic segment; and 2) the total number of individual changes with a frequency greater than 2% in each genomic segment.

1.5 Further details on molecular evolution and phylogenetic methods

Individual orthohantavirus segment sequences were first aligned using MAFFT version 7.397 and analyzed for synonymous and nonsynonymous changes using Geneious version 7.1.3 (www.geneious.com). Segment sequences were also concatenated using Geneious. A maximum-likelihood phylogenetic tree was estimated for individual S-segment and concatenated sequence alignments using PhyML v3.3.[19] PhyML was run using exhaustive search parameters, a General-Time Reversible (GTR) nucleotide substitution model with gamma distributed rate variation among sites, and 1,000 bootstrap replications. The tree was visualized and rooted using FigTree version 1.4.[20]

Individual and concatenated alignments were also used to reconstruct a median-joining haplotype network using PopART v1.7.2 (http://popart.otago.ac.nz) as previously described.[14]

1.6 Further details on multiplex immunological assays

Human cytokine concentrations of 62 serum samples (51 isolates from 32 individual ANDV-caused hantavirus pulmonary syndrome patients, 5 hantavirus pulmonary syndrome patients infected with LECHV, and 6 samples from healthy volunteers) were quantified to have a better understanding of host immunological response dynamics (**Table S9–Table S15**). Samples were collected in the prodromal and cardiopulmonary stages of infection (mean = 5.0 days, 95% CI. 4.3–5.8) and were split into two groups based on the day of sampling: “Days 1–4” and “Days 5–10” as previously described.[21]

Serum and plasma cytokine profiles were established using a 48-Plex Bio-Plex Pro Human Cytokine Screening Panel (Bio-Rad Laboratories, Hercules, CA, USA). Samples were processed according to manufacturer’s instructions. Sample replicates were run on separate plates. The first set of replicates was processed immediately after thawing; the second set was stored at 4°C after thawing and processed 24 h later. All samples were clarified at 10,000 x *g* for 10 min at 4°C immediately prior to processing. Samples were diluted 1:4 in sample diluent HB and assayed immediately. Plates were manually washed with a multichannel pipet for all wash steps. After assay completion, plates were read on the Luminex Flexmap 3D (MiraiBio, San Burno, CA, USA). Data were exported to Bio-Results Generator 3.0 and Bio-Plex Manager (Bio-Rad Laboratories, Hercules, CA, USA). Replicate values from different plates were manually combined and percent coefficient of variation (%CV) was calculated. Data on concentrations of IL-12 (p40), IL-1α, IL-2, and IL-3 were removed due to low quality.

1.7 Further details on statistical methods

Information is available on all 34 cases regarding, age, sex, date of symptom onset, and residential area. Symptom-onset dates, estimated exposure dates, and predicted incubation times for each case were also used to calculate the best-fit serial interval distribution (time interval between symptom onset of a primary case and to the symptom onset of an epidemiologically-linked secondary case, **Figure S4**). The reproductive number (*R*), i.e., the posterior median number of secondary cases per confirmed ANDV-caused hantavirus pulmonary syndrome patient, was estimated by single and multiple weeks on the basis of the Wallinga and Teunis method,[22] which requires incidence data and the serial interval distribution. A 95% credible interval was calculated for all *R* estimates. The individual reproductive number (Z) was determined from observed reporting of epidemiologically linked secondary cases for each patient. For simplicity, transmission events from a secondary case or alternative source cases with low supporting evidence (Patients 20 and 31, orange in **Figure 1C**) were excluded in serial distribution or *R* calculations.

Thirty-three cases with available clinical information (i.e., excluding Patient 21) were divided into groups based on Z. Only transmission events with strong supporting evidence were considered valid (red in **Figure 1C**) and determined downstream superspreader, all spreader, non-superspreader and non-spreader grouping (**Table S2)**. Further comparisons were made by dividing the patients in 2 groups according to the severity of the disease, mild (severity grades 1–2) versus severe (severity grades 3–4) (**Table S8**). Patients were also divided into two groups attending to the outcome of the hantavirus pulmonary syndrome: survivors versus deceased.

The degree and confirmation of secondary spread, illness outcome, disease severity (severity grade), and whether the patient was isolated was categorized and compared with clinical and genetic characteristics. Univariable associations were compared using the nonparametric Wilcoxon rank-sum test or Pearson's product-moment correlation test. Transmission groups, spread using a discrete binary variable of spread versus no spread, spread using a continuous variable (Z), disease severity, and patient outcome groups were separately compared with all available clinical, genetic, and epidemiological data (**Table S1, Table S2, Table S8**). A generalized linear model was used to estimate unadjusted odds ratios for significant ($P<0.05$) univariable associations. A binary response variable denoting whether the patient was a spreader (all spreaders, $Z>1$) or non-spreader ($Z=0$) was used, and the model family was specified as "binomial" (i.e., a logit-link function). The same approach was used for superspreaders ($Z>4$) versus non-superspreaders ($Z<4$). Univariable associations to calculate adjusted odds ratios were implemented using the same generalized linear model. All P values are two-sided.

Biomarker variable importance was quantified using a machine-learning, tree-based *randomForest* analysis[23] (**Table S14**). Five-hundred random trees, 20 randomly sampled variables per split, auto-bootstrap out-of-bag sampling, and Altmann *et al*.'s permutation test[24] were used for testing the model, determining variable importance, and statistical significance. All RF analysis was performed with the *Ranger* software[25] package implemented in R.

1.8 Further details on case isolation and enforced self-quarantine measures

Provincial and national public health authorities coordinated the establishment of isolation for confirmed ANDV cases and self-quarantine for high-risk contacts. High-risk case-contacts were identified as those who were in close contact for more than 30 min with a confirmed and symptomatic ANDV case. Case-contact self-quarantine was imposed around December 31, 2018

(i.e., after identification of Patient 18). In addition, massive social gatherings were prohibited in the affected area. Suspected high-risk contacts were recommended to remain at home and self-quarantine for at least 40 days and were asked to wear N95 respirators in the presence of others. Control measures were lifted in March 2019.

1.9 Gene pathway analysis of biomarker data trends

Gene lists containing only upregulated genes were submitted to Panther Pathway (http://www.pantherdb.org/) and subject to the "Statistical overrepresentation test". Human gene IDs were used as a reference and "GO biological process complete" terms were used for the annotation data set. Fisher's Exact test was used to test for significance. False discovery rate was used for correction. Only GO terms containing more than one gene and had a >50X fold enrichment in observed versus expected were included in the final reported data set (**Table S15**).

Results

2.1 Andes virus detection and diagnostics

Viral load in blood was high in all patients (33/33), ranging from 1.7 x 10^5–1.3 x 10^8 ANDV RNA copies/ml (mean = 5 x 10^7; median = 4.4 x 10^7) (**Table S1**). ANDV-specific IgM was detected in all (33/33) patients in the earliest available serum samples. ANDV-specific IgG was detected in 94% (31/33) of patients. The two IgG-negative patients were Patient 8, who died 4 days after symptom onset and before the development of an IgG response, and Patient 32, who was unavailable for retesting until 148 days after initial blood collection.

2.2 Additional genomic and phylogenomic analyses

No synapomorphic changes were found to be exclusive to ANDV strain Epuyén/18−19, but both Epilink/96 and NRC-6/18. A single M segment synapomorphic change (F216L) shared by Epuyén/18–19 sequences and NRC-6 (2018) occurred in the ectodomain of the ANDV Gn envelope glycoprotein. Four additional synapomorphic changes observed in the M segment (V353I, V499I, T641I, and V1115I) are shared among Epuyén/18–19, Epilink/96, and NRC-6/18 sequences.

ANDV genomic differences between superspreaders versus non-superspreaders, and all spreaders versus non-spreaders were minimal at the consensus level. We compared the viral minority population diversity between samples obtained from related groups to exclude virological differences between them. No significant differences of subclonal single nucleotide polymorphism frequencies or segment diversity were observed between groups or between central and terminal haplotypes (**Figure S2**), as shown in **Figure 1B**.

Discussion: There was no evidence of positive selection in either the Epuyén/18−19 consensus sequences, even within minority populations, over time or between transmissions. Moreover, no differences in viral diversity between superspreaders, all spreaders, non-superspreaders, and non-spreaders were evident, indicating that viral genomic factors did not explain differences in Z or *R*. This finding also suggests genetic conditions that facilitated person-to-person may have been maintained in reservoir rodent host populations prior to the recent cross-species transmission that occurred in October 2018.

Alterations in orthohantavirus Gn and Gc structures could affect virus-receptor interactions, virion entry, and immune responses such as neutralizing antibody production in rodent or human hosts.[26-30] Four additional synapomorphic changes observed in the M segment (V353I, V499I, T641I, and V1115I) are shared among Epuyén/18–19, Epilink/96 and NRC-6/18 sequences. These three strains are all associated with human disease and could be facilitating higher ANDV transmissibility in humans. A comprehensive analysis of the distribution of ANDV in rodents living in areas where person-to-person transmission has been demonstrated is urgently needed to explore whether other viral-host genetic factors are associated with spreading potential.

In addition to their capabilities for sustaining person-to-person transmission, the genomic similarity of the Epuyén/18−19 and Epilink/96 strains suggests that they share the base-line genetic traits for successful between-host (facilitating spillover) and within-host (facilitating person-to-person) transmission, without a need for adaptation to improve viral fitness, while high

contact rates and a sufficient critical community size (social gatherings and extensive contact) fueled early superspreading events.[31-34] The spillover of canine influenza A virus (canine FLUAV) A/H3N8 subtype in dog shelters also demonstrates how contact heterogeneity with little or no adaptive genetic changes results in Z and *R* variability in a more significant manner than the underlying viral fitness, as high canine FLUAV transmission events occur in densely populated dog shelters whereas low FLUAV prevalence is observed in sparsely populated domestic dog populations.[35-37] Further research on ANDV genetic diversity in reservoir rodent populations in endemic areas could help demonstrate that baseline genetic changes were established prior to ANDV spillover.

2.3 Additional clinical presentation and laboratory data

For some patients, additional information regarding their medical history was available:

- Patient 1, a superspreader, did not have outstanding health complications before attendance.
- Patient 2, a superspreader, had recovered from a gastric cancer 2 years prior to ANDV infection. During his stay at the Hospital Zonal de Esquel, a bone marrow infiltration likely related to gastric cancer was detected at the time of hospitalization.
- Patient 3 was diagnosed with Epstein-Barr virus (*Herpesviridae*: *Lymphocryptovirus*) co-infection during his stay at Hospital Zonal de Esquel.
- Patients 8 and 11 had recently recovering from pneumonia, around 10 days before the onset of prodromal ANDV-caused hantavirus pulmonary syndrome symptoms.
- Patient 9, a superspreader, did not have outstanding health complications before attendance.
- Patient 10 had a chronic asthmatic condition.

Hematologic abnormalities thrombocytopenia, lymphopenia, leukocytosis, and neutrophilia were observed in the majority of the cases. In terms of disease severity, 56% (19/34) of patients were considered to have "severe" presentations of ANDV-caused hantavirus pulmonary syndrome. The overall case-fatality rate was 32% (11/34 cases), and the mean time from symptom onset to death was 6.7 days (interquartile range, 4−7 days). Severe cases were associated with higher prevalence of leukocytosis (OR, 3.7; 95% CI. 1.7–10), neutrophilia (OR, 8.8; 95% CI. 2.5–72), lymphopenia (OR, 3.0; 95% CI 1.2–10), thrombocytopenia (OR, 1.9; 95% CI. 1.3–3.3) and elevated LDH enzymatic activities (OR, 1.3; 95% CI. 1.1–1.5) (**Table S1, Table S8**).

2.4 Unique laboratory parameters of superspreaders

Superspreaders were more likely to have a higher viral load (OR, 1.1; 95% CI. 0.9–1.2), AST activity (OR, 1.2; 95% CI. 0.9–1.5), ALT activity (OR, 1.6; 95% CI. 1.1–2.7) and more severe thrombocytopenia (OR, 3.42; 95% CI. 1.1–17) than all other patients (**Table S8**). Increasing Z was also positively correlated with ALT activities (r=0.51; 95% CI. 0.20–0.73) and longer prothrombin response times (r=0.52; 95% CI. 0.16–0.76). Notably superspreader patients presented with respiratory, hepatic, and renal compromises.

2.5 Differential expression of serum cytokines in ANDV-caused hantavirus pulmonary syndrome patients

Four different cytokine profiles were generated and compared: ANDV-infected versus healthy control individuals, ANDV-infected versus LECHV-infected individuals, ANDV-infected superspreader versus ANDV-infected non-superspreader, and ANDV-infected all spreader versus ANDV-infected non-spreaders (**Table S9**, **Table S10**, **Table 3**^). Univariate comparisons revealed significant associations of disease when an increase in certain biomarker concentrations occurred in ANDV-infected patients compared to healthy volunteers (**Table S10**). 23 cytokines were significantly upregulated in ANDV-infected patients, including interferon (IFN)-γ, interleukin (IL)-4, IL-6, IL-16, and tumor necrosis factor (TNF)-α, among others. Conversely, concentrations of TNF-β (OR, 0.062; 95% CI. 0.004–0.38), IL-9 (OR, 0.85; 95% CI. 0.71–0.98), and platelet-derived growth factor-BB (PDGF-BB; OR, 0.74; 95% CI. 0.53–0.96) were less likely to increase with disease and were significantly downregulated compared to healthy controls.

Comparison of ANDV-infected and LECHV-infected patients revealed remarkable differences in several cytokines (such as IL-6, IFN- γ, TNF-β, and IL-9) and chemokines (such as MIP-1α, MIP-1β, RANTES, monocyte chemotactic protein (MCP)-1, tumor necrosis factor-related apoptosis inducing ligand [TRAIL], and GRO-α) (**Table S13**). A Venn diagram comparing ANDV-caused hantavirus pulmonary syndrome cytokine trends to relevant studies is shown in **Figure S7**.

Additional comparisons of disease severity (particularly in earlier clinical samples [Days 1–4], **Table S11**) and age risk (**Table S12**) also revealed significant associations. MIP-1β, TRAIL, SCGF-β, and PDGF-BB concentrations were significantly different when comparing superspreaders to non-superspreaders. Notably, SCGF-β and Z in ANDV Epuyén/18–19 patients were negatively correlated (r=–0.41; 95% CI. –0.61−–0.15).

^The ORs and CIs in **Table 3** were estimated using the following increments: 10 (IL-1β), 500 (IL-18), 20 (IL-13), 50 (IL-10), 100 (MIP-1β), 50 (TRAIL), 500 (PDGF-BB), 100 (GRO-α), 30 (SCF), and 100,000 (SCGF-β).

Discussion: Characterization of the immune response patterns among ANDV-caused hantavirus pulmonary syndrome cases could aid predicting whether a patient has a higher potential to become a superspreader and/or may help understand ANDV-caused hantavirus pulmonary syndrome cytokine dysregulation compared to that of other orthohantaviruses. ANDV-caused hantavirus pulmonary syndrome patients presented with strong indicators of an unregulated cytokine release syndrome (aka “cytokine storm”, **Table S10**). However, we were unable to associate the observed dysregulation with a specific immune phenotype that may have contributed to variation in disease severity and secondary transmission of ANDV-caused hantavirus pulmonary syndrome patients.

The ANDV Epuyén/18–19 serum cytokine profile contrasted some trends observed in LECHV-caused hantavirus pulmonary syndrome patients and additional reports on the dynamic host immune response to infection with South American orthohantaviruses.[21,38] Upregulation of IL-1β (typically associated with Puumala virus-associated hemorrhagic fever with renal syndrome) and Th1-related IFN- γ, coupled with a general lack of induction of IL-12 (p70) and VEGF, provides evidence that ANDV-caused hantavirus pulmonary syndrome pathogenesis may

be unique compared to hantavirus pulmonary syndrome caused by other orthohantaviruses. Serum biomarker trends also differed from Puumala virus-caused hemorrhagic fever with renal syndrome cytokine profiles, which was shown with the downregulation of TNF-β (typically hemorrhagic fever with renal syndrome-associated), IL-9, and PDGF-BB.[38]
The multiple, independent, mechanisms of immune-evasion and pathogenesis that could facilitate ANDV person-to-person transmission should be investigated in greater detail.

Differences between superspreaders and non-superspreaders further demonstrate a mixed cytotoxic response: MIP-1β and TRAIL are elevated compared to healthy subjects and LECHV-infected patients and are believed to influence mononuclear cell trans-endothelial migration and increase cytotoxic lymphocyte-mediated apoptosis. This elevation is coupled with a downregulation of PDGF-BB, suggesting an inhibition of stromal cells and angiogenic factors during ANDV infection. Interestingly, SCGF-β concentrations, a growth factor for primitive hematopoietic progenitor cells, were significantly different in both all spreaders and superspreaders compared to non-spreaders and non-superspreaders respectively. Importantly, SCGF-β's strong but not as pronounced upregulation in LECHV-infected patients could support the negative correlation with Z, suggesting that a reduced upregulation of SCGF-β may be associated with an increase in ANDV superspreading potential.

2.6 Treatment of hantavirus pulmonary syndrome cases

Most of the patients were monitored daily after fever onset. Seven patients with mild respiratory complications were treated with oxygen supplementation. Patients who progressed to severe clinical infection and presented with any sign of hemodynamic and/or severe respiratory compromise were transferred to the intensive care unit (ICU). Treatment generally consisted of inotropic drug administration, maintenance of fluid balance, and/or respiratory intubation. All severe cases (19/33) presented with acute respiratory distress and required mechanical ventilation and hemodynamic support. Patient 25 entered into shock extremely quickly and died before being transferred to ICU. Five patients (28, 30–34) also received ribavirin starting at the first day of fever.

2.7 Potential sexual transmission of ANDV

Sexual transmission was also considered a potential route of ANDV transmission. Patient 2 infecting Patient 9, and Patient 22 infecting Patient 33 were two instances where sexual transmission could have occurred based on epidemiological reporting and relevant time of symptom onset. However, since both cases also transmitted the virus to other non-sexual contacts, we consider that the most probable route of infection was through close respiratory contact.

Supplementary Figures

Figure S1. Maximum-likelihood tree with branch-specific synapomorphic changes.

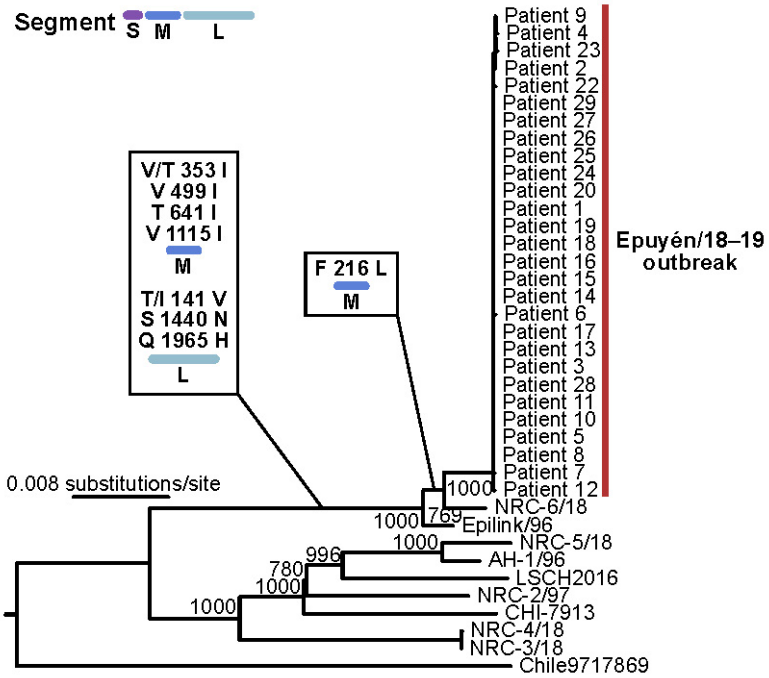

ANDV S, M, and L segments are represented by purple, blue, and cyan bars, respectively. Branches are scaled by substitutions per site. Bootstrap values are found at tree nodes.

Figure S2. Subclonal diversity of ANDV Epuyén/18−19 sequences.

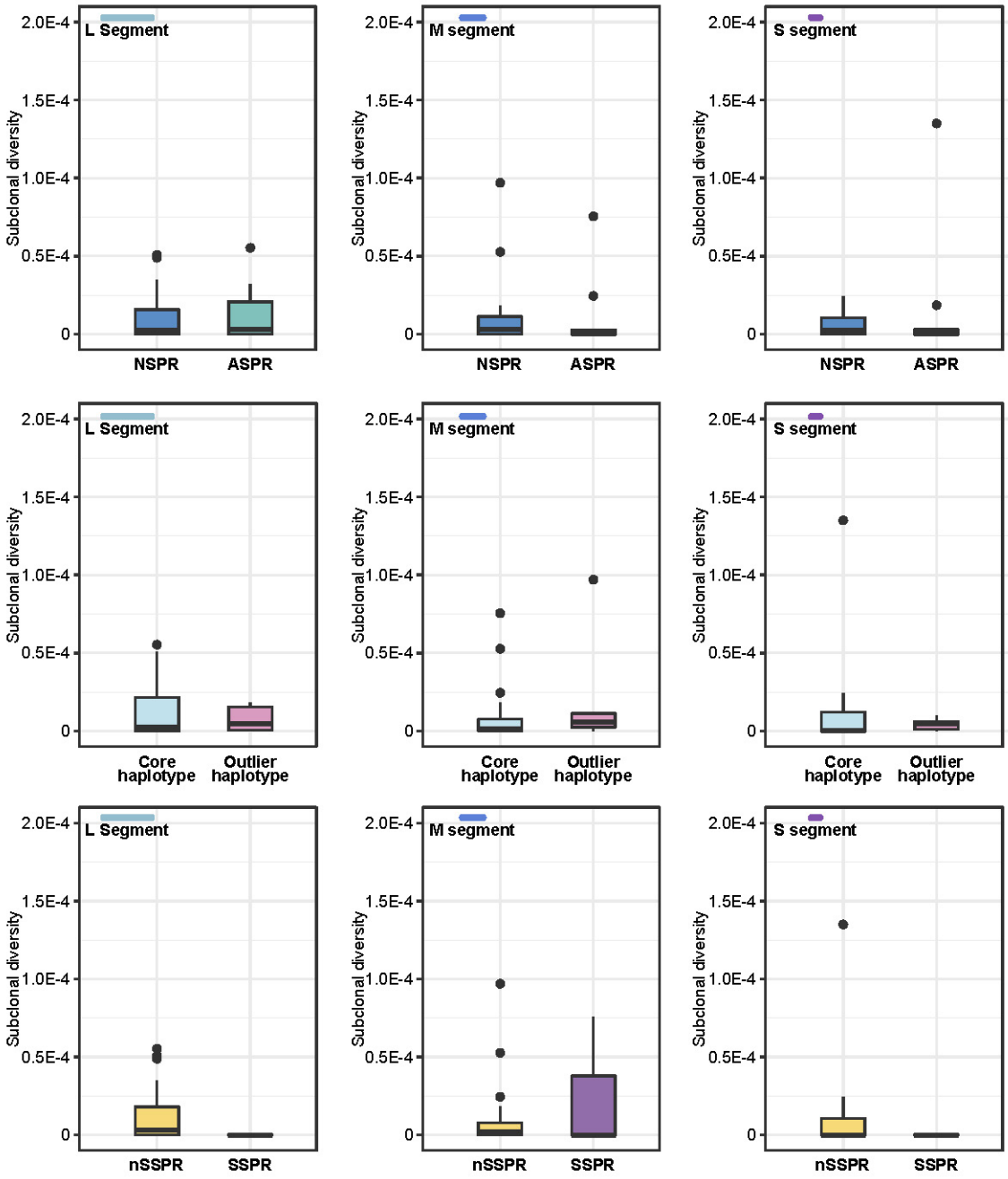

Subclonal diversity is calculated as variants/site/copy are presented as averages across sample groupings for each segment. A Wilcox rank sum test was performed but no significant differences were observed between groupings. Error bars represent standard deviation of the mean. Outliers are represented by black dots. Abbreviations: NSPR, non-spreaders; ASPR, all spreaders; nSSPR, non-superspreader; SSPR, superspreader.

Figure S3. Diagram of first superspreading event at a birthday party

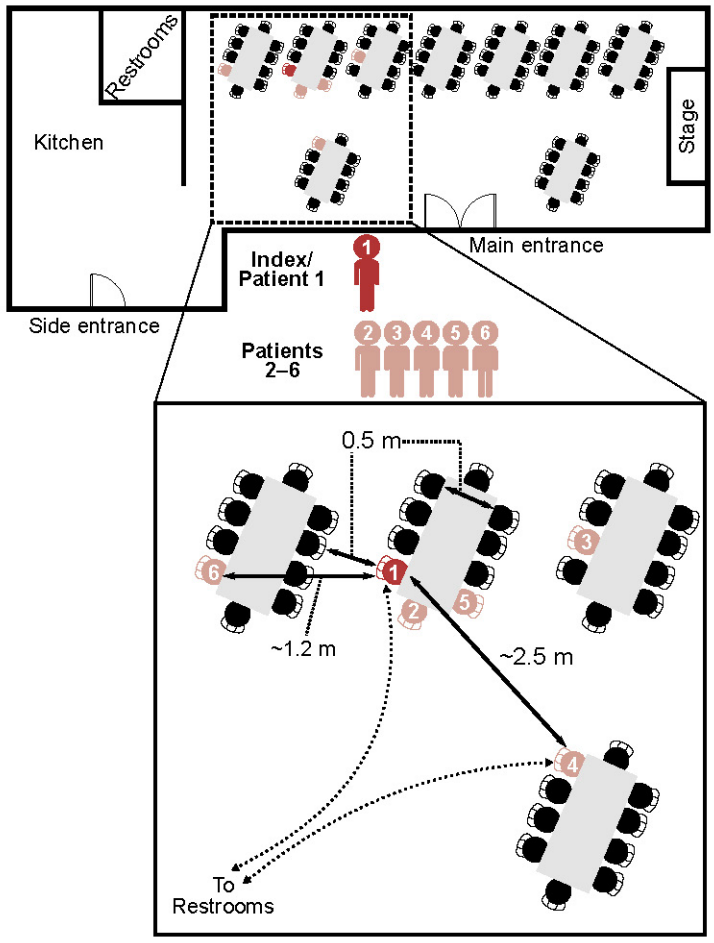

A diagram showing the seating arrangements of a birthday party on November 3, 2018. Over 100 people were reported to have attended the event. The seating locations of Patients 1–6 are shown. Distances between Patient 1 and others are also displayed with solid lines. The two dotted lines demonstrate that Patient 1 and Patient 4 crossed paths on the way to the restroom but did not make any physical contact.

Figure S4. Serial interval distribution of the 2018–2019 ANDV-caused hantavirus pulmonary syndrome outbreak.

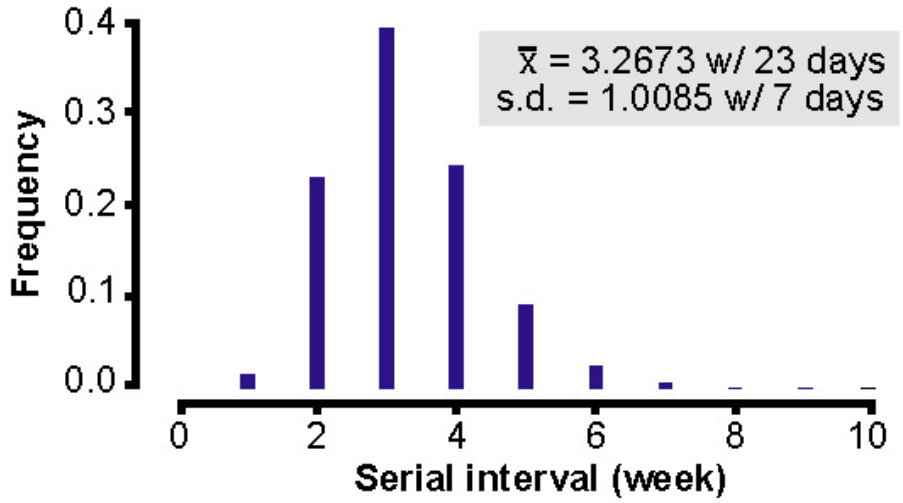

Mean (x) and standard deviation (s.d.) are shown in weeks (w) and days.

Figure S5. Serum biomarkers are significantly dysregulated in spreaders of ANDV-caused hantavirus pulmonary syndrome.

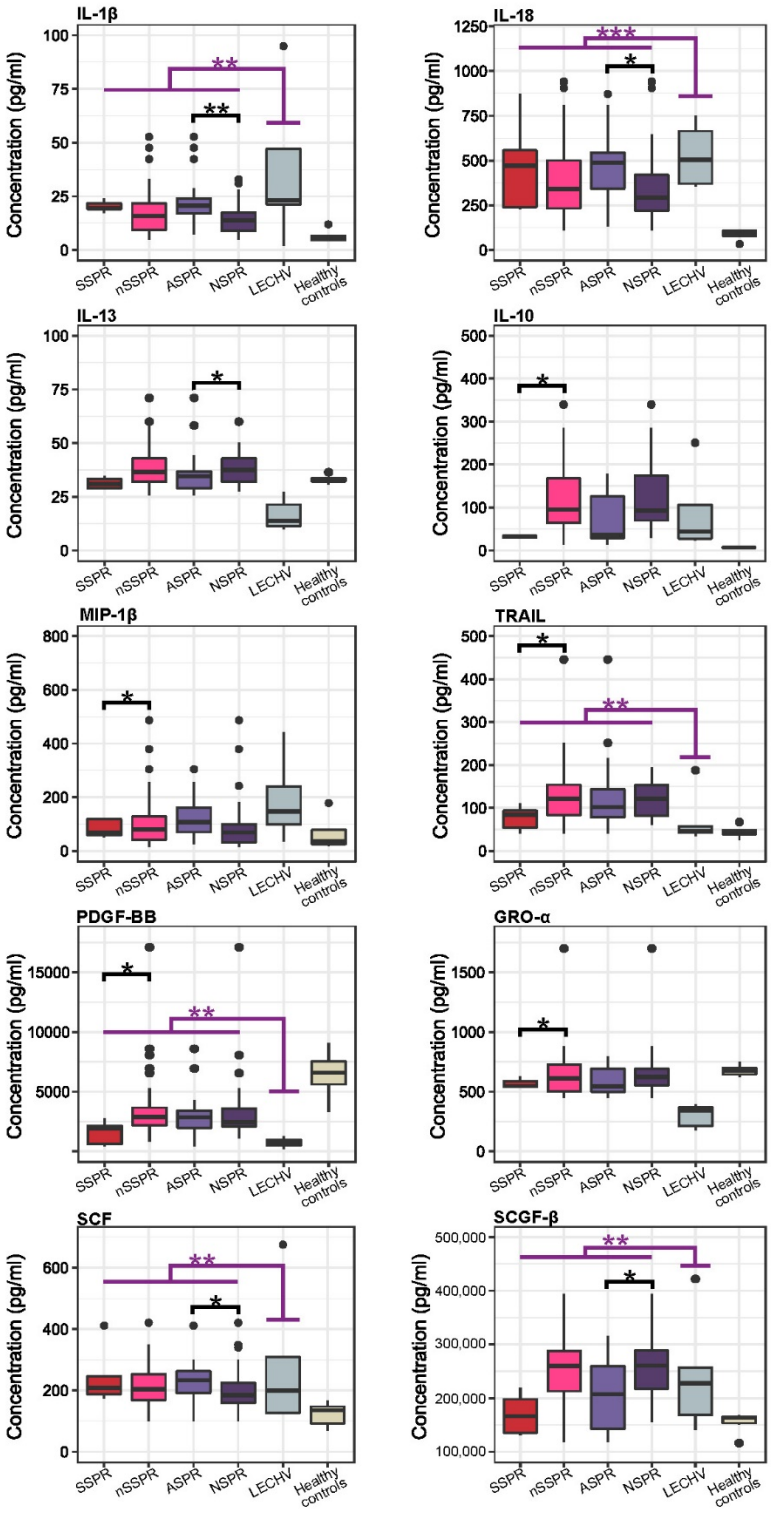

Brackets are shown to signify significant differences between groups. Black brackets compare concentrations of spreader groups: SSPR (superspreaders) versus nSSPR (non-superspreaders),

and ASPR (all spreaders) versus NSPR (non-spreaders). Purple brackets compare Andes virus samples to LECHV (Lechiguanas virus) samples. *P values in between 0.01–0.05. **P values in between 0.0001–0.01. ***P<0.0001. Biomarker concentrations of healthy control serum samples are shown for context; significant differences are not shown here (see Table 3 in the main text). Abbreviations: IL, interleukin; MIP, macrophage inflammatory protein; TRAIL, tumor necrosis factor-related apoptosis inducing ligand; PDGF-BB, platelet-derived growth factor-BB; GRO, growth-regulated oncogene; SCF, stem cell factor; SCGF; stem cell growth factor.

Figure S6. Overview of cytokine trends in ANDV spreaders, ANDV non-spreaders, LECHV-caused hantavirus pulmonary syndrome patients and healthy volunteers.

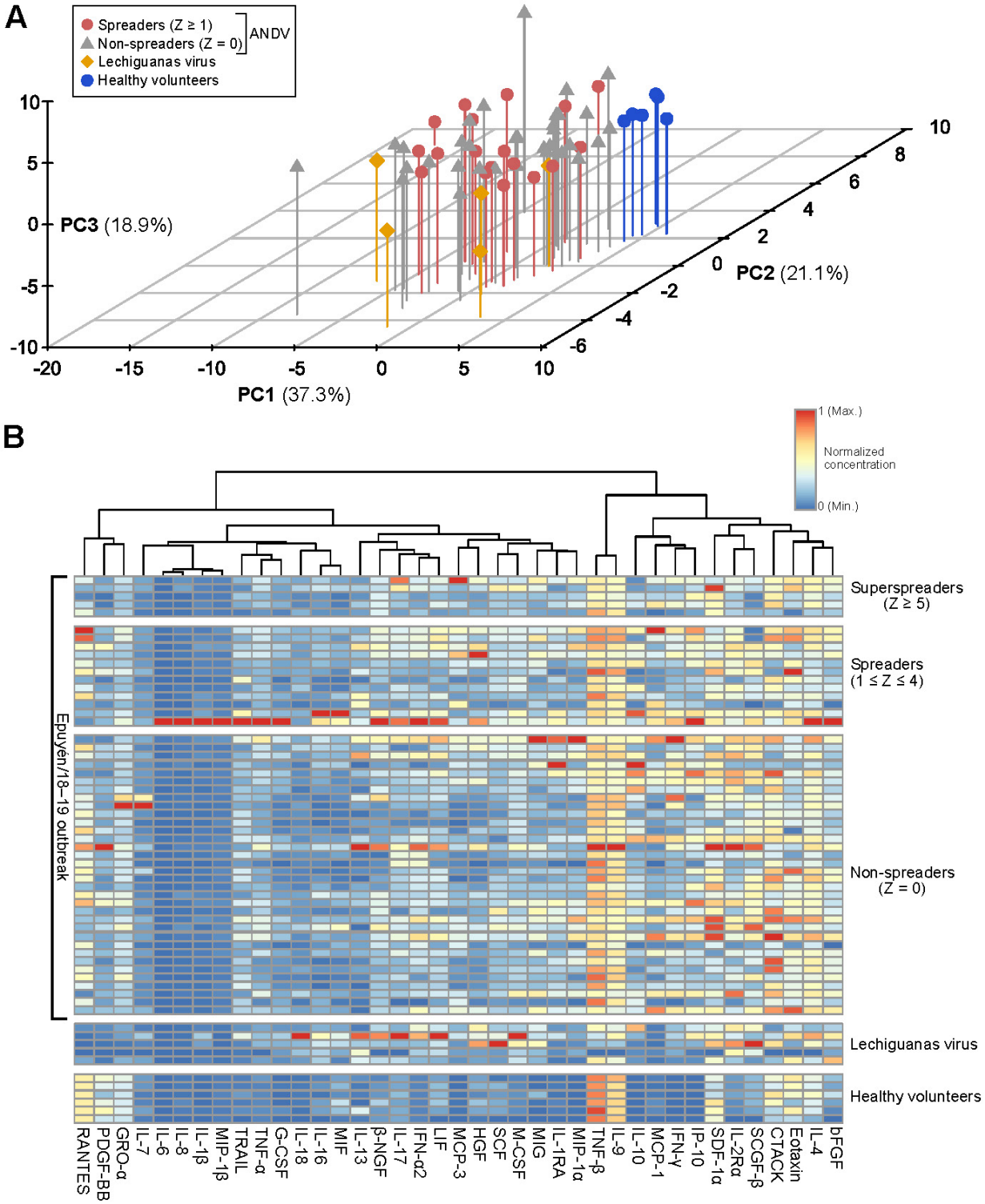

(A) A 3-axis principle component analysis using concentrations of 39 human cytokines. Analytes with more than 20% missing data were removed; missing data in analytes with less than 20% was substituted using a mean value of the respective group. Percentage of principle components (PC) are shown. (B) A heatmap using hierarchical clustering of cytokines and normalized concentrations from 0 (minimum concentration) to 1 (maximum concentration). Rows are spaced by groups based on disease class and the number of secondary transmission events (Z).

Figure S7. Comparing significant changes of 44 serum biomarkers between studies using Venn diagrams.

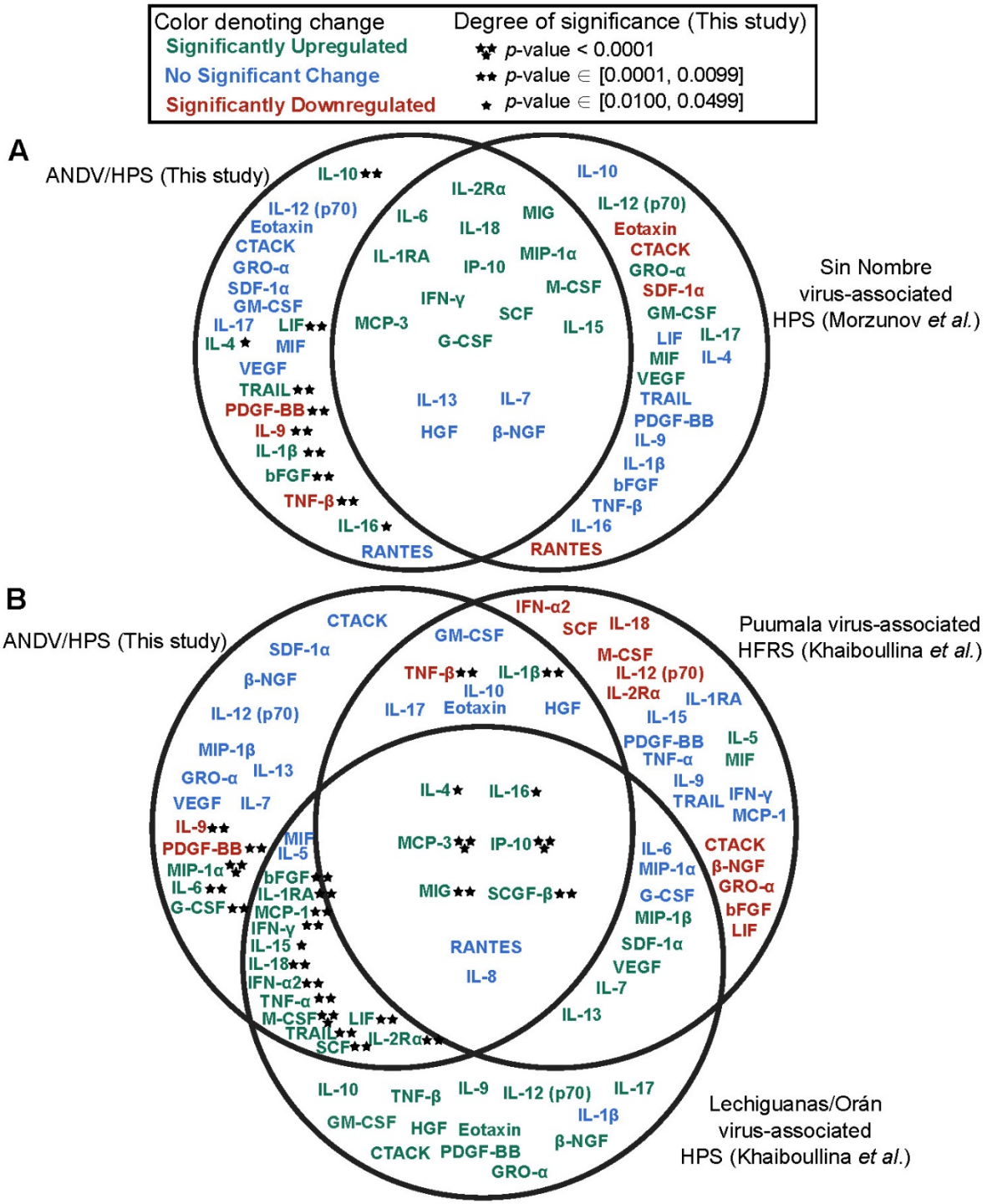

(A) Epuyén/18−19 ANDV-caused hantavirus pulmonary syndrome outbreak patients compared to Sin Nombre virus-casues hantavirus pulmonary syndrome patients described in Morzunov *et al*., 2015. (B) Epuyén/18−19 ANDV-caused hantavirus pulmonary syndrome outbreak patients compared to Puumala virus-associated hemorrhagic fever with renal syndrome (HFRS) and

Lechiguanas/Orán virus-associated hantavirus pulmonary syndrome described in Khaiboullina *et al*., 2017. Colors denoting change and symbols denoting the degree of significance are shown.

Supplementary Tables

Table S1. Complete clinical data from 33 ANDV-caused hantavirus pulmonary syndrome patients. For virologic testing, the earliest possible sample was used for quantification. For serological testing, the most abnormal or elevated values were reported.

See attached Excel file.

Table S2. Epidemiological and individual information on Andes virus-infected patients, November 2018 − February 2019

Patient ID	Age (yr)	Sex	Residence	Probable place of exposure	Exposure date	Fever onset	ANDV HPS case contact#	Relationship	Estimated incubation (d)	Wave of Infection*	Z
Patient 1	68	M	Epuyén	Peridomestic	ND	11/3/2018	-	-	ND	1	5
Patient 2	61	M	Epuyén	Birthday party	11/3/2018	11/23/2018	1	-	20	2	6
Patient 3	15	M	Epuyén	Birthday party	11/3/2018	11/20/2018	1	-	17	2	0
Patient 4	16	M	Epuyén	Birthday party	11/3/2018	11/27/2018	1	-	24	2	0
Patient 5	46	F	Epuyén	Birthday party	11/3/2018	11/26/2018	1	Daughter	23	2	1
Patient 6	14	F	Epuyén	Birthday party	11/3/2018	11/25/2018	1	-	22	2	0
Patient 7	57	M	Epuyén	Work	11/23/2018	12/7/2018	2	Co-worker	14	3	0
Patient 8	72	M	Epuyén	Home	11/23/2018	12/13/2018	2	Friend	20	3	1
Patient 9	43	F	Epuyén	Home	11/23/2018	12/12/2018	2	Wife	19	3	10
Patient 10	38	M	Epuyén	HRE	11/23/2018	12/10/2018	2	-	18	3	3
				HRE	11/20/2018		3	-	15		
				HRE	11/27/2018		4	-	22		
				HRE	11/26/2018		5	-	21		
				HRE	11/25/2018		6	-	20		
Patient 11	65	M	Epuyén	HRE	11/23-24/2018	12/15/2018	2	Co-worker	22	3	0
Patient 12	30	F	Epuyén	Home/HRE	11/23/2018	12/19/2018	2	Daughter	26	3	0
Patient 13	27	M	Epuyén	Home/HRE	11/26/2018	12/24/2018	2	Son	31	3	1
Patient 14	65	F	Epuyén	Home/HRE	11/25/2018	12/26/2018	5	Mother	30	3	1
Patient 15	7	M	Epuyén	Patient 2´s wake	12/12/2018	12/26/2018	9	Nephew	14	4	0
Patient 16	44	F	Epuyén	Patient 2´s wake/shared drink#	12/12/2018	12/28/2018	9	Friend	16	4	0
Patient 17	35	M	Epuyén	Patient 2´s wake/shared drink#	12/12/2018	12/31/2018	9	Brother in law	19	4	0
Patient 18	24	F	Epuyén	Patient 2´s wake/shared drink#	12/12/2018	12/31/2018	9	Sister	19	4	0
Patient 19	36	F	Epuyén	Patient 2´s wake/shared drink#	12/12/2018	1/2/2019	9	Sister	21	4	0

Patient 20	34	F	Trevelin	Meeting in Chile/car trip	12/10/2018	1/1/2019	10	Friend	22	4	0
Patient 21	34	F	Palena	Meeting in Chile	12/10/2018	1/1/2019	10	Friend	22	4	0
Patient 22	58	M	El Maitén	Car Trip	12/12/2018	1/1/2019	9	Neighbor	20	4	3
Patient 23	16	M	Epuyén	Patient 2´s wake	12/12/2018	1/1/2019	9	Son	20	4	0
Patient 24	41	F	El Maitén	Patient 2´s wake	12/12/2018	1/3/2019	9	Sister	22	4	0
Patient 25	32	F	Epuyén	Home/HZE	12/24/2018	1/6/2019	13	Brother	13	4	0
Patient 26	90	F	Epuyén	Home	12/26/2018	1/4/2019	14	Friend	9	4	0
Patient 27	46	F	El Maitén	Patient 2´s wake	12/12/2018	1/8/2019	9	Sister	27	4	0
Patient 28	38	F	El Bolsón	Visited a patient at HZE	12/15/2018	1/7/2019	8	Neighbor	25	4	1
Patient 29	49	F	Trevelin	Home	12/10/2018	1/14/2019	10^	Friend	35	4	0
				Home	1/2/2019		20	Mother	12		
Patient 30	30	M	Epuyén	Patient 2´s wake/Home/Car trip	12/12/2018	1/21/2019	9	Sister	40	4	0
Patient 31	80	M	El Maitén	Car trip	1/1/2019	1/24/2019	22	Neighbor	23	5	0
Patient 32	2	F	El Bolsón	Home	1/7/2019	1/29/2019	28	Grand-daughter	22	5	0
Patient 33	26	F	El Maitén	Home	1/1/2019	2/6/2019	22^	Daughter	36	5	0
				Home	1/24/2019		31	Neighbor	13		
Patient 34	59	F	El Maitén	Home	1/1/2019	2/6/2019	22^	Wife	36	5	0
				Home	1/24/2019		31	Neighbor	13		
Epilink/96	-	F	El Bolsón (RN)	El Bolsón (RN)	1996	11/8/1996	-	-	-	-	-
NRC-2/97	61	M	Bariloche (RN)	Bariloche (RN)	1997	11/26/1997	-	-	-	-	-
NRC-3/18	33	M	VM (NQ)	VM (NQ)	2018	8/15/2018	-	-	-	-	-
NRC-4/18	22	M	VM (NQ)	VM (NQ)	2018	9/6/2018	-	-	-	-	-
NRC-5/18	25	M	Bariloche (RN)	Bariloche (RN)	2018	4/4/2018	-	-	-	-	-
NRC-6/18	26	F	El Bolsón (RN)	El Hoyo (CH)	2018	5/16/2018	-	-	-	-	-

Abbreviations: ANDV, Andes virus; HPS, hantavirus pulmonary syndrome; Z, individual reproductive number; ND, not defined; NRC, not related case; HRE, Hospital Rural de Epuyén; HZE, Hospital Zonal de Esquel; VM, Villa Meliquina; CH, Chubut Province; RN, Río Negro Province; NQ, Neuquén Province. Dates are in month/day/year format. *In a propagated outbreak in which person-to-person transmission can continuously occur, patients are grouped into numerical waves determined by how many times the virus has successfully jumped to a new human host and extended the chain of transmission. Horizontal lines are added when a patient is associated with an alternative source and/or time of infection. [#]patients shared a straw drinking tea with Patient 9. ^Most likely source of infection.

Table S3. Genome percent coverage of sequenced Epuyén/18−19 ANDV genome segments

Patient ID/isolate	Date of extraction	S segment (nt/total [%])	M segment (nt/total [%])	L segment (nt/total [%])
Patient 1	01/28/19	1851/1876 [98.67]	3654/3679 [99.32]	6541/6562 [99.68]
Patient 2	01/28/19	1804/1876 [96.16]	3118/3679 [84.75]	3080/6562 [46.94]
Patient 3	01/28/19	1851/1876 [98.67]	3654/3679 [99.32]	6539/6562 [99.65]
Patient 4	01/28/19	1856/1876 [98.93]	3659/3679 [99.46]	6542/6562 [99.70]
Patient 5	01/28/19	1849/1876 [98.56]	3649/3679 [99.18]	6540/6562 [99.66]
Patient 6	01/28/19	1866/1876 [99.47]	3669/3679 [99.73]	6546/6562 [99.76]
Patient 7	01/28/19	1856/1876 [98.93]	3655/3679 [99.35]	6544/6562 [99.73]
Patient 8	01/28/19	1858/1876 [99.04]	3654/3679 [99.32]	6543/6562 [99.71]
Patient 9	01/28/19	1867/1876 [99.52]	3669/3679 [99.73]	6549/6562 [99.80]
Patient 10	01/28/19	1843/1876 [98.24]	3639/3679 [98.91]	6415/6562 [97.76]
Patient 11	01/28/19	1844/1876 [98.29]	3645/3679 [99.08]	6522/6562 [99.39]
Patient 12	01/28/19	1852/1876 [98.72]	3655/3679 [99.35]	6542/6562 [99.70]
Patient 13	01/28/19	1851/1876 [98.67]	3657/3679 [99.40]	6541/6562 [99.68]
Patient 14	01/28/19	1855/1876 [98.88]	3658/3679 [99.43]	6543/6562 [99.71]
Patient 15	01/28/19	1828/1876 [97.44]	3633/3679 [98.75]	6531/6562 [99.53]
Patient 16	01/28/19	1859/1876 [99.09]	3651/3679 [99.24]	6541/6562 [99.68]
Patient 17	01/28/19	1861/1876 [99.20]	3659/3679 [99.46]	6543/6562 [99.71]
Patient 18	01/28/19	1826/1876 [97.33]	3633/3679 [98.75]	6490/6562 [98.90]
Patient 19	01/28/19	1865/1876 [99.41]	3656/3679 [99.37]	6547/6562 [99.77]
Patient 20	01/28/19	1862/1876 [99.25]	3655/3679 [99.35]	6539/6562 [99.65]
Patient 22	01/28/19	1863/1876 [99.31]	3661/3679 [99.51]	6546/6562 [99.76]
Patient 23	01/28/19	1850/1876 [98.61]	3646/3679 [99.10]	6531/6562 [99.53]
Patient 24	01/28/19	1849/1876 [98.56]	3652/3679 [99.27]	6532/6562 [99.54]
Patient 25	01/28/19	1861/1876 [99.20]	3654/3679 [99.32]	6542/6562 [99.70]
Patient 26	01/28/19	1858/1876 [99.04]	3654/3679 [99.32]	6541/6562 [99.68]
Patient 27	01/28/19	1848/1876 [98.51]	3647/3679 [99.13]	6533/6562 [99.56]
Patient 28	01/28/19	1849/1876 [98.56]	3647/3679 [99.13]	6532/6562 [99.54]
Patient 29	01/28/19	1861/1876 [99.20]	3665/3679 [99.62]	6542/6562 [99.70]

Table S4. Information on all sequences used in this study

Species	Variant	Strain	Patient ID/Isolate	Date of sampling	Sampling place	Sample Type	S segment*	M segment*	L segment*
Andes orthohantavirus	Andes virus	Epuyén/18–19	Patient 1	11/10/2018	Esquel, Chubut, ARG	Whole Blood	MN258239	MN258205	MN258172
Andes orthohantavirus	Andes virus	Epuyén/18–19	Patient 2	11/28/2018	Esquel, Chubut, ARG	Whole Blood	MN258249	MN258215	-
Andes orthohantavirus	Andes virus	Epuyén/18–19	Patient 3	11/26/2018	Esquel, Chubut, ARG	Whole Blood	MN258250	MN258216	MN258182
Andes orthohantavirus	Andes virus	Epuyén/18–19	Patient 4	12/3/2018	Esquel, Chubut, ARG	Whole Blood	MN258251	MN258217	MN258183
Andes orthohantavirus	Andes virus	Epuyén/18–19	Patient 5	12/9/2018	Esquel, Chubut, ARG	Whole Blood	MN258252	MN258218	MN258184
Andes orthohantavirus	Andes virus	Epuyén/18–19	Patient 6	12/2/2018	Esquel, Chubut, ARG	Whole Blood	MN258253	MN258219	MN258185
Andes orthohantavirus	Andes virus	Epuyén/18–19	Patient 7	12/12/2018	Esquel, Chubut, ARG	Whole Blood	MN258254	MN258220	MN258186
Andes orthohantavirus	Andes virus	Epuyén/18–19	Patient 8	12/16/2018	Esquel, Chubut, ARG	Whole Blood	MN258255	MN258221	MN258187
Andes orthohantavirus	Andes virus	Epuyén/18–19	Patient 9	12/14/2018	Esquel, Chubut, ARG	Whole Blood	MN258256	MN258222	MN258188
Andes orthohantavirus	Andes virus	Epuyén/18–19	Patient 10	12/15/2018	Esquel, Chubut, ARG	Whole Blood	MN258229	MN258195	MN258162
Andes orthohantavirus	Andes virus	Epuyén/18–19	Patient 11	12/19/2018	Esquel, Chubut, ARG	Whole Blood	MN258230	MN258196	MN258163
Andes orthohantavirus	Andes virus	Epuyén/18–19	Patient 12	12/21/2018	Esquel, Chubut, ARG	Whole Blood	MN258231	MN258197	MN258164
Andes orthohantavirus	Andes virus	Epuyén/18–19	Patient 13	12/24/2018	Esquel, Chubut, ARG	Whole Blood	MN258232	MN258198	MN258165
Andes orthohantavirus	Andes virus	Epuyén/18–19	Patient 14	12/28/2018	Esquel, Chubut, ARG	Whole Blood	MN258233	MN258199	MN258166
Andes orthohantavirus	Andes virus	Epuyén/18–19	Patient 15	12/28/2018	Esquel, Chubut, ARG	Whole Blood	MN258234	MN258200	MN258167
Andes orthohantavirus	Andes virus	Epuyén/18–19	Patient 16	1/1/2019	Esquel, Chubut, ARG	Whole Blood	MN258235	MN258201	MN258168
Andes orthohantavirus	Andes virus	Epuyén/18–19	Patient 17	1/3/2019	Esquel, Chubut, ARG	Whole Blood	MN258236	MN258202	MN258169
Andes orthohantavirus	Andes virus	Epuyén/18–19	Patient 18	1/2/2019	Esquel, Chubut, ARG	Whole Blood	MN258237	MN258203	MN258170

Andes orthohantavirus	Andes virus	Epuyén/18–19	Patient 19	1/2/2019	Bariloche, Río Negro, ARG	Whole Blood	MN258238	MN258204	MN258171
Andes orthohantavirus	Andes virus	Epuyén/18–19	Patient 20	1/6/2019	Esquel, Chubut, ARG	Whole Blood	MN258240	MN258206	MN258173
Andes orthohantavirus	Andes virus	Epuyén/18–19	Patient 22	1/4/2019	Esquel, Chubut, ARG	Whole Blood	MN258241	MN258207	MN258174
Andes orthohantavirus	Andes virus	Epuyén/18–19	Patient 23	1/5/2019	Esquel, Chubut, ARG	Whole Blood	MN258242	MN258208	MN258175
Andes orthohantavirus	Andes virus	Epuyén/18–19	Patient 24	1/6/2019	Esquel, Chubut, ARG	Whole Blood	MN258243	MN258209	MN258176
Andes orthohantavirus	Andes virus	Epuyén/18–19	Patient 25	1/6/2019	Esquel, Chubut, ARG	Whole Blood	MN258244	MN258210	MN258177
Andes orthohantavirus	Andes virus	Epuyén/18–19	Patient 26	1/7/2019	Esquel, Chubut, ARG	Whole Blood	MN258245	MN258211	MN258178
Andes orthohantavirus	Andes virus	Epuyén/18–19	Patient 27	1/10/2019	Esquel, Chubut, ARG	Whole Blood	MN258246	MN258212	MN258179
Andes orthohantavirus	Andes virus	Epuyén/18–19	Patient 28	1/10/2019	Bariloche, Río Negro, ARG	Whole Blood	MN258247	MN258213	MN258180
Andes orthohantavirus	Andes virus	Epuyén/18–19	Patient 29	1/16/2019	Esquel, Chubut, ARG	Whole Blood	MN258248	MN258214	MN258181
Andes orthohantavirus	Andes virus	Epilink/96	Epilink/96	12/11/1996	Ciudad de Buenos Aires, ARG	Whole Blood	MN258223	MN258189	MN258156
Andes orthohantavirus	Andes virus	NRC-2/97	NRC-2/97	11/30/1997	Bariloche, Río Negro, ARG	Whole Blood	MN258224	MN258190	MN258157
Andes orthohantavirus	Andes virus	NRC-3/18	NRC-3/18	11/9/2018	San Martín de los Andes, Neuquén, ARG	Whole Blood	MN258225	MN258191	MN258158
Andes orthohantavirus	Andes virus	NRC-4/18	NRC-4/18	8/19/2018	San Martín de los Andes, Neuquén, ARG	Whole Blood	MN258226	MN258192	MN258159
Andes orthohantavirus	Andes virus	NRC-5/18	NRC-5/18	9/4/2018	Bariloche, Río Negro, ARG	Whole Blood	MN258227	MN258193	MN258160
Andes orthohantavirus	Andes virus	NRC-6/18	NRC-6/18	5/21/2018	Bariloche, Río Negro, ARG	Whole Blood	MN258228	MN258194	MN258161
Andes orthohantavirus	Andes virus	AH-1	AH-1	1996	ARG	Lung tissue	AF324902.1	AF324901.2	-
Andes orthohantavirus	Andes virus	LSCH2016	LSCH2016	2016	CHE (exported from CHL)	Whole Blood	KY659432.1	KY604962.1	KY659431.1

Andes orthohantavirus	Andes virus	CHI-7913	CHI-7913	1999	CHL	Whole Blood	AY228237.1	AY228238.1	AY228239.1
Andes orthohantavirus	Andes virus	Chile9717869	Chile R123	1997	CHL	Whole Blood	AF291702.1	AF291703.2	AF291704.5
Andes orthohantavirus	Bermejo virus	Oc22531	Oc22531	1997	Orán, ARG	Rodent tissue	AF482713.1	-	-
Andes orthohantavirus	Lechiguanas virus	22819	22819	1997	Lechiguanas Islands, ARG	Rodent tissue	AF482714.1	-	-
Andes orthohantavirus	Orán virus	22996	22996	1997	Orán, ARG	Rodent tissue	AF482715.1	-	-
Andes orthohantavirus	Maciel virus	13796	13796	1997	Maciel, ARG	Rodent tissue	AF482716.1	-	-
Andes orthohantavirus	Castelo dos Sonhos virus	Castelo dos Sonhos virus-2	AN717313/BRA300	2006	Campo Novo dos Parecis, BRA	Whole Blood	JX443691.1	-	-
Andes orthohantavirus	Pergamino virus	14403	14403	1997	Pergamino, ARG	Rodent tissue	AF482717.1	-	-
Sin Nombre orthohantavirus	-	NM H10	Case H10	1993	New Mexico, USA	Whole Blood	L25784.1	-	-

*GenBank accession numbers

Table S5. Pairwise percent identity of a concatenated alignment using S and M segments from 28 ANDV Epuyén/18−19 isolates

	Patient 1	Patient 5	Patient 6	Patient 3	Patient 4	Patient 2	Patient 14	Patient 7	Patient 9	Patient 8	Patient 12	Patient 11	Patient 10	Patient 17	Patient 15	Patient 18	Patient 13	Patient 19	Patient 16	Patient 23	Patient 22	Patient 20	Patient 29	Patient 28	Patient 25	Patient 26	Patient 27	Patient 24
Patient 1		100	100	100	100	100	100	99.9	100	100	100	100	100	100	100	100	100	100	100	99.9	99.9	100	100	100	100	100	100	100
Patient 5	100		100	100	100	100	100	99.9	100	100	100	100	100	100	100	100	100	100	100	99.9	99.9	100	100	100	100	100	100	100
Patient 6	100	100		100	100	100	100	99.9	100	100	100	100	100	100	100	100	100	100	100	99.9	99.9	100	100	100	100	100	100	100
Patient 3	100	100	100		100	100	100	99.9	100	100	100	100	100	100	100	100	100	100	100	99.9	99.9	100	100	100	100	100	100	100
Patient 4	100	100	100	100		100	100	99.9	100	100	100	100	100	100	100	100	100	100	100	99.9	99.9	100	100	100	100	100	100	100
Patient 2	100	100	100	100	100		100	99.9	100	100	100	100	100	100	100	100	100	100	100	99.9	99.9	100	100	100	100	100	100	100
Patient 14	100	100	100	100	100	100		99.9	100	100	100	100	100	100	100	100	100	100	100	99.9	99.9	100	100	100	100	100	100	100
Patient 7	99.9	99.9	99.9	99.9	99.9	99.9	99.9		99.9	99.9	99.9	99.9	99.9	99.9	99.9	99.9	99.9	99.9	99.9	99.8	99.9	99.9	99.9	99.9	99.9	99.9	99.9	99.9
Patient 9	100	100	100	100	100	100	100	99.9		100	100	100	100	100	100	100	100	100	100	99.9	99.9	100	100	100	100	100	100	100
Patient 8	100	100	100	100	100	100	100	99.9	100		100	100	100	100	100	100	100	100	100	99.9	99.9	100	100	100	100	100	100	100
Patient 12	100	100	100	100	100	100	100	99.9	100	100		100	100	100	100	100	100	100	100	99.9	99.9	100	100	100	100	100	100	100
Patient 11	100	100	100	100	100	100	100	99.9	100	100	100		100	100	100	100	100	100	100	99.9	99.9	100	100	100	100	100	100	100
Patient 10	100	100	100	100	100	100	100	99.9	100	100	100	100		100	100	100	100	100	100	99.9	99.9	100	100	100	100	100	100	100
Patient 17	100	100	100	100	100	100	100	99.9	100	100	100	100	100		100	100	100	100	100	99.9	99.9	100	100	100	100	100	100	100
Patient 15	100	100	100	100	100	100	100	99.9	100	100	100	100	100	100		100	100	100	100	99.9	99.9	100	100	100	100	100	100	100
Patient 18	100	100	100	100	100	100	100	99.9	100	100	100	100	100	100	100		100	100	100	99.9	99.9	100	100	100	100	100	100	100
Patient 13	100	100	100	100	100	100	100	99.9	100	100	100	100	100	100	100	100		100	100	99.9	99.9	100	100	100	100	100	100	100
Patient 19	100	100	100	100	100	100	100	99.9	100	100	100	100	100	100	100	100	100		100	99.9	99.9	100	100	100	100	100	100	100
Patient 16	100	100	100	100	100	100	100	99.9	100	100	100	100	100	100	100	100	100	100		99.9	99.9	100	100	100	100	100	100	100
Patient 23	99.9	99.9	99.9	99.9	99.9	99.9	99.9	99.8	99.9	99.9	99.9	99.9	99.9	99.9	99.9	99.9	99.9	99.9	99.9		99.8	99.9	99.9	99.9	99.9	99.9	99.9	99.9
Patient 22	99.9	99.9	99.9	99.9	99.9	99.9	99.9	99.9	99.9	99.9	99.9	99.9	99.9	99.9	99.9	99.9	99.9	99.9	99.9	99.8		99.9	99.9	99.9	99.9	99.9	99.9	99.9
Patient 20	100	100	100	100	100	100	100	99.9	100	100	100	100	100	100	100	100	100	100	100	99.9	99.9		100	100	100	100	100	100
Patient 29	100	100	100	100	100	100	100	99.9	100	100	100	100	100	100	100	100	100	100	100	99.9	99.9	100		100	100	100	100	100
Patient 28	100	100	100	100	100	100	100	99.9	100	100	100	100	100	100	100	100	100	100	100	99.9	99.9	100	100		100	100	100	100
Patient 25	100	100	100	100	100	100	100	99.9	100	100	100	100	100	100	100	100	100	100	100	99.9	99.9	100	100	100		100	100	100
Patient 26	100	100	100	100	100	100	100	99.9	100	100	100	100	100	100	100	100	100	100	100	99.9	99.9	100	100	100	100		100	100
Patient 27	100	100	100	100	100	100	100	99.9	100	100	100	100	100	100	100	100	100	100	100	99.9	99.9	100	100	100	100	100		100
Patient 24	100	100	100	100	100	100	100	99.9	100	100	100	100	100	100	100	100	100	100	100	99.9	99.9	100	100	100	100	100	100	

Table S6. Positions of nucleotide differences and amino acid changes from ANDV RefSeq strain (GenBank accessions AF291702–4) to ANDV Epuyén/18−19 sequences.

Segment	Nucleotide position	Nucleotide change	Amino acid position	Amino acid change	Genome with change
S	19	T → C			
S	21	G → A			
S	24	G → A			
S	78	G → A			
S	93	A → G			
S	130	C → T			
S	177	A → G			
S	183	T → C			
S	198	A → G			
S	202	T → C			
S	219	A → G			
S	264	T → C			
S	270	A → G			
S	273	G → A			
S	276	A → G			
S	315	T → C			
S	321	T → C			
S	324	T → C			
S	375	C → T			
S	402	C → A			
S	408	G → A			
S	412	T → C			
S	417	C → T			
S	432	T → C			
S	456	C → T			
S	462	G → A			
S	465	C → T			
S	534	C → T			
S	546	A → G			
S	558	C → T			
S	591	A → T			
S	615	T → C			
S	618	T → C			
S	636	C → T			
S	642	T → C			
S	651	T → C			
S	666	A → G			
S	687	A → G			
S	693	T → C			
S	711	A → G			
S	714	G → A			
S	717	T → C			
S	740	T → C	247	Ser → Leu	Patient 7
S	741	A → G			
S	756	C → T			
S	783	T → C			

S	795	T → C			
S	837	T → C			
S	843	C → T			
S	855	C → T			
S	864	G → A			
S	867	C → T			
S	888	A → G			
S	891	G → A			
S	930	A → G			
S	963	T → C			
S	975	G → A			
S	990	T → C			
S	996	T → C			
S	999	C → T			
S	1,068	A → G			
S	1,083	C → T			
S	1,089	A → T			
S	1,095	A → G			
S	1,101	G → A			
S	1,116	A → G			
S	1,119	C → T			
S	1,131	G → A			
S	1,146	T → C			
S	1,155	A → T			
S	1,182	C → T			
S	1,215	C → A			
S	1,233	T → C			
S	1,242	T → C			
S	1,245	T → C			
S	1,278	T → A			
M	23	T → C	8	Val → Ala	All
M	63	G → A			
M	108	C → A			
M	123	C → T			
M	139	C → T			
M	141	A → G			
M	180	C → T			
M	192	C → T			
M	213	A → G			
M	273	T → C			
M	288	G → A			
M	294	T → C			
M	309	A → G			
M	312	T → C			
M	324	A → C	108	Lys → Asn	All
M	336	T → C			
M	343	C → T			
M	357	C → T			
M	363	T → C			
M	366	A → G			
M	381	A → G			
M	396	C → T			

M	403	C → T			
M	411	T → C			
M	417	A → G			
M	457	AT → GC			
M	474	A → T			
M	495	G → T			
M	519	T → C			
M	582	C → T			
M	592	T → C			
M	600	G → A			
M	618	T → C			
M	630	T → G			
M	646	T → C	216	Phe → Leu	All
M	669	A → G			
M	705	G → A			
M	720	G → A			
M	735	G → A			
M	747	G → A			
M	786	G → A			
M	790	T → C			
M	819	T → C			
M	849	A → G			
M	858	T → C			
M	867	G → A			
M	876	A → G			
M	880	C → T	294	His → Tyr	All
M	885	A → G			
M	945	G → A			
M	981	T → C			
M	987	T → G			
M	999	A → G			
M	1,020	A → G			
M	1,032	T → G			
M	1,036	AG → CA	346	Val → Ile	All
M	1,041	T → G			
M	1,050	T → C			
M	1,053	C → T			
M	1,058	C → T	353	Thr → Ile	All
M	1,071	G → A			
M	1,146	T → C			
M	1,155	A → G			
M	1,158	A → G			
M	1,173	T → C			
M	1,179	G → A			
M	1,191	A → G			
M	1,200	A → C			
M	1,203	T → C			
M	1,209	C → T			
M	1,215	T → C			
M	1,242	A → G			
M	1,249	C → A			
M	1,251	T → A			

M	1,254	A → G			
M	1,266	A → G			
M	1,281	T → C			
M	1,302	T → C			
M	1,323	A → G			
M	1,347	T → A			
M	1,359	G → A			
M	1,362	G → A			
M	1,417	T → C			
M	1,419	G → A			
M	1,434	T → C			
M	1,440	G → A			
M	1,446	A → G			
M	1,471	C → T			
M	1,479	A → C			
M	1,488	T → C			
M	1,495	G → A	499	Val → Ile	All
M	1,509	G → A			
M	1,512	C → A			
M	1,530	G → A			
M	1,536	A → G			
M	1,548	G → A			
M	1,609	A → G	537	Ile → Val	All
M	1,615	G → T	539	Asp → Tyr	All
M	1,620	A → G			
M	1,644	C → T			
M	1,677	A → G			
M	1,698	G → A			
M	1,704	T → C			
M	1,707	C → T			
M	1,719	T → C			
M	1,725	T → C			
M	1,749	T → C			
M	1,752	A → G			
M	1,779	T → C			
M	1,794	A → G			
M	1,812	G → A			
M	1,827	A → G			
M	1,863	C → A			
M	1,873	A → C			
M	1,875	A → C			
M	1,878	T → C			
M	1,917	G → A			
M	1,922	C → T	641	Thr → Ile	All
M	1,926	T → C			
M	1,944	C → T			
M	1,963	C → T			
M	1,977	C → T			
M	1,989	G → A			
M	2,026	C → T			
M	2,028	C → A			
M	2,034	G → A			

M	2,044	C → T			
M	2,064	C → T			
M	2,070	T → C			
M	2,094	C → T			
M	2,097	T → C			
M	2,100	A → G			
M	2,154	A → G			
M	2,164	C → T			
M	2,166	G → A			
M	2,184	G → A			
M	2,190	T → C			
M	2,208	T → C			
M	2,274	G → A			
M	2,337	A → G			
M	2,340	C → T			
M	2,358	T → C			
M	2,361	C → T			
M	2,379	T → G			
M	2,382	G → A			
M	2,397	A → C			
M	2,412	T → C			
M	2,427	T → C			
M	2,451	T → A			
M	2,472	T → C			
M	2,484	G → A			
M	2,499	A → G			
M	2,502	T → C			
M	2,523	A → T			
M	2,550	G → A			
M	2,577	A → G			
M	2,583	T → C			
M	2,589	G → A			
M	2,646	C → T			
M	2,667	G → A			
M	2,682	T → C			
M	2,703	T → C			
M	2,812	A → G	938	Thr → Ala	All
M	2,817	C → T			
M	2,832	C → T			
M	2,844	G → A			
M	2,859	C → T			
M	2,865	C → T			
M	2,886	C → T			
M	2,916	T → C			
M	2,926	C → T			
M	2,928	A → G			
M	2,967	A → C			
M	2,979	C → T			
M	3,009	A → G			
M	3,030	G → A			
M	3,042	A → T			
M	3,067	A → G	1023	Thr → Ala	All

M	3,081	G → A			
M	3,111	A → G			
M	3,117	C → T			
M	3,129	C → T			
M	3,168	A → G			
M	3,172	T → C			
M	3,174	A → T			
M	3,189	T → A			
M	3,201	G → A			
M	3,210	A → C			
M	3,222	T → C			
M	3,264	A → T			
M	3,282	T → C			
M	3,294	G → A			
M	3,321	T → C			
M	3,343	G → A	1115	Val → Ile	All
M	3,363	T → C			
M	3,382	T → C			
M	3,384	G → C			
M	3,387	T → C			
M	3,399	G → A			
M	3,414	C → T			
L	12	T → C			
L	18	G → A			
L	39	C → T			
L	51	A → G			
L	54	G → A			
L	96	C → T			
L	108	T → C			
L	112	CC → TT			
L	114	G → A			
L	120	C → T			
L	147	T → C			
L	165	A → G			
L	183	A → G			
L	262	AT → GC			
L	267	A → G			
L	291	T → C			
L	303	T → C			
L	306	A → C			
L	309	T → C			
L	312	C → T			
L	351	G → A			
L	390	A → T			
L	396	C → T			
L	417	G → T			
L	422	AAC → GGT	141	Thr → Val	All
L	441	T → C			
L	453	T → C			
L	474	G → A			
L	477	T → G			
L	507	G → A			

L	513	G → A			
L	519	C → T			
L	525	G → A			
L	573	A → T			
L	591	T → C			
L	619	TT → AC			
L	624	G → A			
L	633	T → C			
L	642	G → A			
L	651	A → G			
L	664	C → T			
L	675	T → C			
L	723	C → T			
L	780	A → G			
L	825	A → G			
L	830	T → C	277	Leu → Ser	All
L	834	T → C			
L	849	C → T			
L	858	A → G			
L	864	A → G			
L	909	A → G			
L	915	A → G			
L	924	T → C			
L	966	A → C			
L	981	A → G			
L	1,005	G → A			
L	1,012	T → G	338	Ser → Ala	All
L	1,029	T → C			
L	1,037	G → A	346	Lys → Arg	All
L	1,047	G → A			
L	1,050	C → T			
L	1,053	T → C			
L	1,062	C → T			
L	1,083	G → A			
L	1,089	T → C			
L	1,091	A → G	364	Asn → Ser	All
L	1,095	G → A			
L	1,104	A → G			
L	1,111	C → T			
L	1,113	G → A			
L	1,143	C → G			
L	1,155	T → C			
L	1,188	A → G			
L	1,194	A → G			
L	1,206	C → T			
L	1,215	C → T			
L	1,224	G → A			
L	1,278	A → T			
L	1,323	T → C			
L	1,341	T → C			
L	1,351	C → T			
L	1,356	A → G			

L	1,383	T → G
L	1,435	C → T
L	1,473	T → C
L	1,476	G → T
L	1,482	C → T
L	1,494	T → C
L	1,503	A → G
L	1,539	C → T
L	1,555	C → T
L	1,557	A → G
L	1,560	G → A
L	1,596	T → C
L	1,599	A → G
L	1,602	T → C
L	1,611	G → A
L	1,617	A → T
L	1,620	C → T
L	1,623	A → G
L	1,626	T → C
L	1,641	G → A
L	1,644	C → T
L	1,653	T → C
L	1,659	C → T
L	1,662	C → T
L	1,677	G → A
L	1,689	T → C
L	1,702	T → C
L	1,707	G → A
L	1,710	T → C
L	1,716	C → T
L	1,722	T → C
L	1,746	G → A
L	1,749	T → A
L	1,824	C → T
L	1,836	C → A
L	1,848	A → G
L	1,857	G → A
L	1,863	T → C
L	1,914	C → T
L	1,923	C → T
L	1,926	G → A
L	1,930	T → C
L	1,953	A → G
L	1,992	C → T
L	1,998	A → G
L	2,004	A → G
L	2,055	T → C
L	2,079	C → T
L	2,082	C → T
L	2,088	C → T
L	2,106	C → T
L	2,130	T → C

L	2,133	C → T			
L	2,139	T → C			
L	2,149	T → C			
L	2,169	T → C			
L	2,206	T → C			
L	2,220	T → C			
L	2,253	G → A			
L	2,259	C → T			
L	2,271	A → G			
L	2,280	T → C			
L	2,338	G → A	780	Asp → Asn	All
L	2,355	T → C			
L	2,364	G → A			
L	2,370	C → T			
L	2,391	G → A			
L	2,394	C → T			
L	2,404	T → C			
L	2,409	G → A			
L	2,433	T → C			
L	2,448	A → G			
L	2,457	C → T			
L	2,466	T → C			
L	2,469	C → T			
L	2,490	T → C			
L	2,493	C → T			
L	2,505	T → C			
L	2,508	G → T			
L	2,520	G → A			
L	2,526	A → G			
L	2,544	G → A			
L	2,550	G → A			
L	2,565	G → A			
L	2,583	A → G			
L	2,586	C → T			
L	2,616	G → A			
L	2,626	T → G	876	Ser → Ala	All
L	2,649	T → C			
L	2,691	C → T			
L	2,716	T → C			
L	2,718	A → G			
L	2,721	A → G			
L	2,772	T → C			
L	2,796	A → G			
L	2,847	A → G			
L	2,868	C → T			
L	2,922	C → A			
L	2,943	T → C			
L	2,952	T → C			
L	2,955	G → A			
L	2,958	T → C			
L	2,988	C → T			
L	3,004	AC → GT			

L	3,006	G → A			
L	3,033	T → C			
L	3,036	C → T			
L	3,054	T → C			
L	3,063	C → T			
L	3,066	G → A			
L	3,097	A → G	1033	Asn → Asp	All
L	3,111	G → A			
L	3,120	T → C			
L	3,129	A → G			
L	3,135	C → T			
L	3,159	A → G			
L	3,168	C → T			
L	3,183	C → T			
L	3,201	A → G			
L	3,252	G → A			
L	3,270	T → C			
L	3,306	G → A			
L	3,309	C → T			
L	3,324	G → A			
L	3,378	G → A			
L	3,426	C → T			
L	3,444	G → A			
L	3,447	C → T			
L	3,462	T → C			
L	3,465	T → C			
L	3,495	A → G			
L	3,501	T → C			
L	3,528	T → C			
L	3,552	C → T			
L	3,555	T → C			
L	3,567	C → A			
L	3,573	G → A			
L	3,576	T → C			
L	3,618	A → G			
L	3,630	A → G			
L	3,649	C → T			
L	3,651	A → G			
L	3,657	G → A			
L	3,672	A → G			
L	3,693	A → G			
L	3,744	A → G			
L	3,771	G → A			
L	3,783	C → T			
L	3,813	A → G			
L	3,828	G → A			
L	3,849	G → A			
L	3,909	T → A	1303	Asp → Glu	All
L	3,918	G → A			
L	3,921	C → T			
L	3,924	A → C			
L	3,975	C → T			

L	3,984	G → A			
L	4,020	A → G			
L	4,026	C → T			
L	4,065	A → G			
L	4,083	G → A			
L	4,131	A → G			
L	4,137	T → C			
L	4,155	A → G			
L	4,182	T → C			
L	4,209	A → G			
L	4,215	T → C			
L	4,221	C → T			
L	4,230	A → G			
L	4,233	A → G			
L	4,236	G → A			
L	4,314	T → C			
L	4,317	G → A			
L	4,319	G → A	1440	Ser → Asn	All
L	4,326	A → G			
L	4,377	T → C			
L	4,401	C → T			
L	4,440	A → G			
L	4,482	A → G			
L	4,515	T → C			
L	4,518	G → T			
L	4,521	G → A			
L	4,527	C → T			
L	4,548	G → A			
L	4,566	T → C			
L	4,587	A → G			
L	4,594	C → T			
L	4,599	T → C			
L	4,620	A → G			
L	4,650	T → C			
L	4,665	A → G			
L	4,669	CC → TT			
L	4,677	C → T			
L	4,686	A → G			
L	4,725	G → T			
L	4,740	A → G			
L	4,773	C → T			
L	4,788	G → A			
L	4,800	C → T			
L	4,821	G → A			
L	4,825	C → T			
L	4,845	T → C			
L	4,854	A → G			
L	4,869	G → A			
L	4,896	A → G			
L	4,914	A → G			
L	4,941	T → C			
L	4,944	A → G			

L	4,960	C → T			
L	4,962	G → A			
L	4,977	G → A			
L	5,022	T → G			
L	5,031	T → C			
L	5,043	A → G			
L	5,055	A → G			
L	5,088	G → T			
L	5,130	A → G			
L	5,151	A → G			
L	5,154	A → G			
L	5,190	T → C			
L	5,202	T → C			
L	5,212	T → C			
L	5,249	A → G	1750	Lys → Arg	All
L	5,253	G → A			
L	5,271	T → G			
L	5,289	G → A			
L	5,299	AC → GT			
L	5,325	A → G			
L	5,355	G → A			
L	5,358	A → G			
L	5,415	T → C			
L	5,427	G → A			
L	5,454	C → T			
L	5,466	G → A			
L	5,469	T → C			
L	5,475	G → A			
L	5,490	T → C			
L	5,520	T → C			
L	5,523	T → G			
L	5,553	G → A			
L	5,571	A → G			
L	5,590	C → T			
L	5,604	A → G			
L	5,610	A → G			
L	5,616	G → A			
L	5,622	A → G			
L	5,664	T → C			
L	5,667	T → C			
L	5,676	T → C			
L	5,688	G → A			
L	5,745	C → T			
L	5,748	C → A			
L	5,766	G → A			
L	5,796	G → A			
L	5,826	C → T			
L	5,895	G → C	1965	Gln → His	All
L	5,934	T → A			
L	5,940	T → C			
L	5,949	C → T			
L	5,952	T → C			

L	5,961	A → G			
L	5,964	G → A			
L	6,000	G → A			
L	6,009	A → G			
L	6,012	C → T			
L	6,015	T → C			
L	6,051	G → A			
L	6,063	A → G			
L	6,072	G → A			
L	6,075	T → C			
L	6,078	A → G			
L	6,087	T → G			
L	6,090	G → A			
L	6,114	C → T			
L	6,129	C → T			
L	6,144	C → T			
L	6,156	C → T			
L	6,174	C → T			
L	6,255	C → T			
L	6,282	G → A			
L	6,300	A → G			
L	6,325	A → G	2109	Val → Ile	All
L	6,351	A → G			
L	6,354	G → A			
L	6,363	G → A			
L	6,399	C → T			
L	6,420	G → A			
L	6,432	C → T			

Table S7. Evidence(s) for possible inhalation exposure during the Epuyén/18−19 ANDV-caused hantavirus pulmonary syndrome outbreak

Infected Patient	Exposed Patient(s)	Event
Patient 1	Patient 4	Birthday party; did not have any physical contact and simply said “hello” to each other as they crossed paths. The spatial distance between individuals during this interaction is unknown.
Patient 1	Patients 3 & 6	Birthday party; seated at different tables and spatially separated by 1–2 m. This distance between the infectees and infector suggests that droplet inhalation transmission is more likely than small droplet aerosol, since no other guests were infected that were seated beyond neighboring tables.
Patients 2, 3, 4, 5 & 6	Patient 10	Administrator at the Epuyén Rural Hospital. Epuyén Rural Hospital is a very small hospital (described to be about the size of a small single-family house); the size is a likely factor of more frequent and closer exposures among admitted patients. Patient 10 did not report having any close or physical contact with other ANDV-infected patients but frequently entered and exited rooms in which infected patients were present. There is also the possibility that an infected patient may have approached Patient 10 to seek medical attention from a healthcare worker.
Patient 2	Patient 11	Patient 2 reported to Epuyén Rural Hospital on the night of fever onset and was admitted to a room that was shared by Patient 11. Patient 11 was admitted for unrelated pneumonia and developed ANDV-caused hantavirus pulmonary syndrome symptoms 22 days later. No direct or close contact between the two patients was reported.
Patient 8	Patient 28	On December 13, 2018, Patient 28 visited Esquel Zonal Hospital where a relative of hers had been admitted as a suspected ANDV-caused hantavirus pulmonary syndrome case (the relative was later found negative for the virus). Patient 8 reported first symptoms on the same day and was admitted to Esquel Zonal Hospital. Patient 8 shared a room with Patient 28 and her relative. Patient 28 and Patient 8 did were not in close contact. Importantly, Patient 8 was using a respirator incorrectly, which may have contributed to Patient 28’s exposure to the virus.

Table S8. Statistical comparisons of ANDV-caused hantavirus pulmonary syndrome patient serological, epidemiological and demographic data.

See attached excel file.

Table S9. Complete biomarker data from 62 serum samples

See attached excel file.

Table S10. Serum cytokine profiles of Andes virus Epuyén/18–19 hantavirus pulmonary syndrome patients and healthy volunteers

Biomarkers	All days (mean ± SD [pg/ml])					
Cytokines	**Epuyén/18–19 (n = 51)**	**Controls (n = 6)**	**Odds ratio[#] (95% CI)**	**Increments**	**P value[&]**	**Changes in serum**
IL-2Rα	409.64 ± 184.48	128.35 ± 33.08	1.7 (1.2–3.5)	10	<0.001	Upregulated
IL-6	131.44 ± 654.58	4.69 ± 3.16	1.4 (1.1–2.2)	1.0	<0.001	Upregulated
IFN-α2*	29.79 ± 9.53	17.92 ± NA	1.7 (0.98–7.8)	1.0	0.13	
IFN-γ	106.36 ± 60.14	8.05 ± 1.54	1.0 (0.79–2.5)	0.0010	0.02	Upregulated
IL-1RA	5949.53 ± 4106.20	675.90 ± 312.07	1.4 (1.1–2.3)	100	<0.001	Upregulated
IL-16	313.59 ± 258.95	151.31 ± 70.04	2.7 (1.1–11)	100	0.04	Upregulated[$]
TNF-β	401.47 ± 61.57	486.8 ± 24.45	0.062 (0.0040–0.38)	100	0.002	Downregulated
IL-5	1092.43 ± 1384.98	78.90 ± 55.18	1.1 (1.0–2.4)	10	0.57	
GM-CSF	15.95 ± 13.31	6.91 ± 3.61	1.5 (1.0–3.0)	1.0	0.1	
TNF-α	202.42 ± 95.64	92.82 ± 8.62	1.1 (1.0–1.3)	1.0	<0.001	Upregulated
IL-1β	26.23 ± 59.07	6.38 ± 2.90	1.8 (1.2–3.5)	1.0	<0.001	Upregulated
IL-18	395.86 ± 213.95	87.64 ± 29.62	12.7 (1.1–Inf)	1.0	<0.001	Upregulated
IL-13	13.21 ± 12.08	8.38 ± 9.39	1.1 (0.96–1.3)	1.0	0.26	
IL-4	7.89 ± 1.80	6.06 ± 1.29	2.4 (1.2–6.2)	1.0	0.02	Upregulated
IL-8	130.06 ± 364.62	82.48 ± 48.6	1.1 (0.85–NA)	100	0.65	
IL-10*	116.27 ± 79.50	7.16 ± NA	1.0 (0.80–2.0)	0.0010	0.1	
IL-15	502.50 ± 150.88	279.71 ± 20.11	1.0 (0.98–1.2)	10	0.02	Upregulated
IL-7	41.21 ± 40.09	27.99 ± 8.53	1.1 (1.0–1.1)	1.0	0.22	
IL-12 (p70)*	14.45 ± 15.85	7.46 ± NA	1.1 (1.0–1.7)	0.1	0.25	
IL-17	24.91 ± 9.14	18.59 ± 1.39	2.5 (0.94–10)	5.0	0.07	
IL-9	331.56 ± 55.73	386.10 ± 15.13	0.85 (0.71–0.98)	10	0.008	Downregulated
Chemokines						
MIG	6176.73 ± 3976.29	803.04 ± 1500.98	4.5 (1.9–18.7)	1000	<0.001	Upregulated
MIP-1β	393.95 ± 663.84	264.21 ± 15.68	3.7 (1.1–44)	100	0.22	
SDF-1α	669.39 ± 196.32	615.43 ± 117.28	1.2 (0.75–2.1)	100	0.51	
MCP-3	16.58 ± 12.67	1.74 ± 0.54	4.9 (1.6–52)	1.0	<0.001	Upregulated
LIF	200.93 ± 74.53	131.66 ± 28.11	1.4 (1.1–2.0)	10	0.01	Upregulated
MIF	2991.80 ± 2851.00	3123.93 ± 1564.04	0.98 (0.77–1.5)	1000	0.36	
RANTES*	13705.68 ± 7755.44	22216.90 ± NA	0.90 (0.70–1.1)	1000	0.21	
Eotaxin	90.15 ± 36.84	91.41 ± 28.29	1.0 (0.98–1.0)	1.0	0.73	
IP-10	29119.08 ± 17229.23	315.52 ± 174.30	1.0 (0.67–7.4)	1.0	<0.001	Upregulated
MCP-1	586.23 ± 487.76	89.19 ± 44.39	9.8 (2.2–103)	100	<0.001	Upregulated
MIP-1α	23.40 ± 14.97	3.36 ± 0.31	2.0 (1.2–15)	0.10	<0.001	Upregulated
TRAIL	122.26 ± 65.37	43.63 ± 14.05	3.2 (1.6–10)	10	<0.001	Upregulated
CTACK	887.40 ± 351.86	709.37 ± 224.63	1.2 (0.91–1.6)	100	0.19	
Growth Factors						
Basic FGF	97.53 ± 20.68	69.68 ± 13.02	2.8 (1.5–6.5)	10	0.002	Upregulated
VEGF	538.68 ± 750.31	312.63 ± 64.19	1.1 (0.93–2.2)	100	0.72	
β-NGF	4.72 ± 2.08	2.85 ± 0.78	3.2 (1.1–21)	1.0	0.03	Upregulated

PDGF-BB	3264.15 ± 2613.45	6460.11 ± 1988.30	0.74 (0.53–0.96)	1000	0.002	Downregulated
G-CSF	235.05 ± 187.66	78.34 ± 29.77	1.6 (1.2–2.6)	10	<0.001	Upregulated
GRO-α	644.07 ± 207.02	677.77 ± 46.20	0.99 (0.96–1.0)	10	0.15	
HGF	1591.19 ± 1217.51	902.53 ± 375.83	1.1 (0.99–1.4)	100	0.16	Upregulated^
SCF	213.98 ± 71.22	122.84 ± 38.96	1.4 (1.1–1.9)	10	0.001	Upregulated
M-CSF	129.83 ± 45.69	34.05 ± 10.96	1.6 (1.1–4.1)	1.0	<0.001	Upregulated
SCGF-β	238762.25 ± 66376.59	154560.48 ± 19826.99	22 (2.8–590)	100000	0.003	Upregulated

Abbreviations: IL-2Rα, interleukin 2 receptor subunit alpha; IL, interleukin; IFN, interferon; TNF-β, tumor necrosis factor beta; GM-CSF, granulocyte-macrophage colony-stimulating factor; p70, protein 70; MIG, monokine induced by gamma interferon; MIP, macrophage inflammatory protein; SDF, stromal cell-derived factor 1; MCP, monocyte chemotactic protein; LIF, leukemia inhibitory factor; MIF, macrophage migration inhibitory factor; RANTES, regulated upon activation normal T cell expressed and secreted; IP-10, interferon gamma-induced protein 10; TRAIL, tumor necrosis factor-related apoptosis inducing ligand; CTACK, cutaneous T-cell-attracting chemokine; bFGF, basic fibroblast growth factor; VEGF; vascular endothelial growth factor; NGF, nerve growth factor; PDGF-BB, platelet-derived growth factor-BB; G-CSF, granulocyte-colony stimulating factor; GRO, growth-regulated oncogene; HGF, human growth factor; SCF, stem cell factor; M-CSF, macrophage colony-stimulating factor; SCGF-β, stem cell growth factor beta; CI, confidence interval; Inf, infinite value. *Insufficient data in control group prevented a calculated standard deviation. [$]Significant upregulated in ANDV samples collected 5–10 days after symptom onset (P=0.006). ^Significant upregulated in ANDV samples collected 5–10 days after symptom onset (P=0.02). [#]Odds ratios with 95% confidence intervals were estimated for the association between elevated concentrations of biomarkers and Andes virus Epuyén/18–19 hantavirus pulmonary syndrome patients compared to healthy volunteers. [&]P values refer to the rank-sum test between variables.

Table S11. Biomarker expression differences and severity in ANDV-caused hantavirus pulmonary syndrome patients

Biomarkers	**All days (mean ± SD [pg/ml])**					**Days 1–4**		
Cytokines	**Severe disease^ (n=23)**	**Mild disease> (n=28)**	**Odds ratio (95% CI)#**	**Increment**	**P value&**	**Odds ratio (95% CI)#**	**Increment**	**P value&**
TNF-β	389.48 ± 63.68	416.06 ± 56.87	0.48 (0.18–1.2)	100	0.07	0.1 (0.0090–0.56)	100	0.007
Chemokines								
SDF-1α	755.63 ± 198.87	564.40 ± 134.4	2.1 (1.4–3.6)	100	<0.001	3.0 (1.5–8.9)	100	0.003
IP-10	32289.05 ± 15222.72	25259.98 ± 19023.54	1.0 (1.0–1.0)	1.0	0.05	1.0 (1.0–1.0)	1.0	0.02
Growth Factors								
VEGF*	320.75 ± NA	829.25 ± NA	0.84 (0.54–1.0)	100	0.11	0.20 (0.014–0.76)	100	0.01
GRO-α	595.90 ± 118.25	702.72 ± 271.46	0.97 (0.92–1.0)	10	0.11	0.92 (0.84–0.99)	10	0.02
HGF	1842.74 ± 1281.15	1284.95 ± 1084.43	1.1 (0.99–1.1)	100	0.03	1.1 (0.92–1.3)	100	0.28
SCGF-β	256516.60 ± 69508.85	217148.27 ± 56517.01	2.6 (1.1–7.4)	100000	0.04	2.2 (0.52–10)	100000	0.23

Abbreviations: TNF-β, tumor necrosis factor beta; SDF, stromal cell-derived factor; IP-10, interferon gamma-induced protein 10; VEGF, vascular endothelial growth factor; NGF, nerve growth factor; GRO, growth-regulated oncogene; HGF, human growth factor; SCF, stem cell factor; SCGF-β, stem cell growth factor beta; CI, confidence interval. *Insufficient data prevented a calculable standard deviation. ^Patients with Severity Grade III or Grade IV. >Patients with Severity Grade I or Grade II. #Odds ratios with 95% confidence intervals were estimated for the association between elevated concentrations of biomarkers and severe disease presentations of Andes virus Epuyén/18–19 hantavirus pulmonary syndrome compared to mild presentations. &P values refer to the rank-sum test between variables.

Table S12. Biomarker expression differences and age risk in ANDV-caused hantavirus pulmonary syndrome patients

Biomarkers	**All days (mean ± SD [pg/ml])**				
Cytokines	**High risk age^ (n=17)**	**Low risk age (n=34)**	**Odds ratio (95% CI)[#]**	**Increment**	**P value[&]**
IL-16*	206.47 ± NA	368.87 ± NA	0.55 (0.29–0.88)	100	0.006
Chemokines					
MIP-1β	269.01 ± 46.25	456.42 ± 809.07	0.24 (0.055–0.77)	100	0.02
IP-10	22670.13 ± 15461.48	32343.55 ± 17370.2	1.0 (1.0–1.0)	10	0.03
Growth Factors					
PDGF-BB	2234.38 ± 899.47	3779.04 ± 3022.74	0.55 (0.29–0.89)	1000	0.01

Abbreviations: IL-16, interleukin 16; MIP, macrophage inflammatory protein; IP-10, interferon gamma-induced protein 10; PDGF-BB, platelet-derived growth factor-BB; CI, confidence interval. *Insufficient data in control group prevented a calculated standard deviation. ^Patients that were <6 or >60 years of age were considered high risk patients. [#]Odds ratios with 95% confidence intervals were estimated for the association between elevated concentrations of biomarkers and risk age group. [&]P values refer to the rank-sum test between variables.

Table S13. Biomarker expression differences between ANDV Epuyén/18–19- and LECHV-infected patients

Biomarkers	All days (mean ± SD [pg/ml])				LECHV vs Controls	Significant changes in serum	
Cytokines	**Epuyén/18–19**	**LECHV**	**P value***	**Controls**	**P value**	**LECHV**	**ANDV**
IL-2Rα	409.64 ± 184.48	486.40 ± 200.96	<0.001	128.35 ± 33.08	0.004	Upregulated	Upregulated
IL-6	131.44 ± 654.58	12.57 ± 8.23	<0.001	4.69 ± 3.16	0.03	Upregulated	Upregulated
IFN-α2*	29.79 ± 9.53	32.09 ± NA	0.92	17.92 ± NA	0.50		
IFN-γ	106.36 ± 60.14	49.56 ± 18.57	0.02	8.05 ± 1.54	0.10		Upregulated
IL-1RA	5949.53 ± 4106.20	2408.92 ± 2380.42	<0.001	675.90 ± 312.07	0.01	Upregulated	Upregulated
IL-16*	313.59 ± 258.95	509.21 ± NA	0.04	151.31 ± 70.04	0.01	Upregulated	Upregulated
TNF-β	401.47 ± 61.57	226.62 ± 112.79	0.002	486.8 ± 24.45	0.004	Downregulated	Downregulated
IL-5*	1092.43 ± 1384.98	73.59 ± NA	0.38	78.90 ± 55.18	1.00		
GM-CSF*	15.95 ± 13.31	14.12 ± NA	0.10	6.91 ± 3.61	0.63		
TNF-α	202.42 ± 95.64	129.45 ± 44.79	<0.001	92.82 ± 8.62	0.13		Upregulated
IL-1β	26.23 ± 59.07	37.65 ± 35.81	<0.001	6.38 ± 2.90	0.13		Upregulated
IL-18	395.86 ± 213.95	1149.84 ± 1397.06	<0.001	87.64 ± 29.62	0.004	Upregulated	Upregulated
IL-13*	13.21 ± 12.08	24.05 ± NA	0.26	8.38 ± 9.39	0.34		
IL-4	7.89 ± 1.80	6.12 ± 3.48	0.02	6.06 ± 1.29	0.79		Upregulated
IL-8	130.06 ± 364.62	40.74 ± 6.96	0.65	82.48 ± 48.60	0.13		
IL-10*	116.27 ± 79.50	90.30 ± NA	0.10	7.16 ± NA	0.40		
IL-15*	502.50 ± 150.88	458.94 ± NA	0.02	279.71 ± 20.11	0.50		Upregulated
IL-7	41.21 ± 40.09	32.12 ± 22.87	0.22	27.99 ± 8.53	0.93		
IL-12 (p70)*	14.45 ± 15.85	11.71 ± 6.74	0.25	7.46 ± NA	0.67		
IL-17	24.91 ± 9.14	27.70 ± 19.98	0.07	18.59 ± 1.39	0.41		
IL-9	331.56 ± 55.73	214.08 ± 95.18	0.008	386.10 ± 15.13	0.004	Downregulated	Downregulated
Chemokines							
MIG	6176.73 ± 3976.29	6474.04 ± 2976.98	<0.001	803.04 ± 1500.98	0.009	Upregulated	Upregulated
MIP-1β	393.95 ± 663.84	133.59 ± 58.80	0.22	264.21 ± 15.68	0.004	Downregulated	
SDF-1α	669.39 ± 196.32	613.69 ± 231.70	0.51	615.43 ± 117.28	0.79		
MCP-3	16.58 ± 12.67	10.48 ± 6.06	<0.001	1.74 ± 0.54	0.008	Upregulated	Upregulated
LIF*	200.93 ± 74.53	269.20 ± NA	0.01	131.66 ± 28.11	0.17		Upregulated
MIF	2991.80 ± 2851	3894.99 ± 2256.21	0.36	3123.93 ± 1564.04	0.66		
RANTES*	13705.68 ± 7755.44	2321.37 ± 2030.98	0.21	22216.90 ± NA	0.33		

Eotaxin	90.15 ± 36.84	74.70 ± 46.49	0.73	91.41 ± 28.29	0.79		
IP-10	29119.08 ± 17229.23	16994.89 ± 16276.62	<0.001	315.52 ± 174.3	0.004	Upregulated	Upregulated
MCP-1	586.23 ± 487.76	89.64 ± 29.68	<0.001	89.19 ± 44.39	1.00		Upregulated
MIP-1α	23.40 ± 14.97	10.31 ± 3.22	<0.001	3.36 ± 0.31	0.008	Upregulated	Upregulated
TRAIL	122.26 ± 65.37	73.60 ± 64.28	<0.001	43.63 ± 14.05	0.43		Upregulated
CTACK	887.40 ± 351.86	479.58 ± 361.72	0.19	709.37 ± 224.63	0.25		
Growth Factors							
Basic FGF	97.53 ± 20.68	102.24 ± 33.62	0.002	69.68 ± 13.02	0.05		Upregulated
VEGF*	538.68 ± 750.31	527.58 ± NA	0.72	312.63 ± 64.19	0.04	Upregulated	
β-NGF*	4.72 ± 2.08	4.86 ± NA	0.03	2.85 ± 0.78	0.49		Upregulated
PDGF-BB	3264.15 ± 2613.45	717.97 ± 403.61	0.002	6460.11 ± 1988.30	0.004	Downregulated	Downregulated
G-CSF	235.05 ± 187.66	215.07 ± 86.80	<0.001	78.34 ± 29.77	0.004	Upregulated	Upregulated
GRO-α	644.07 ± 207.02	299.12 ± 97.95	0.15	677.77 ± 46.20	0.004	Downregulated	
HGF	1591.19 ± 1217.51	2567.05 ± 1720.32	0.16	902.53 ± 375.83	0.13		Upregulated^
SCF	213.98 ± 71.22	287.28 ± 229.22	0.001	122.84 ± 38.96	0.25		Upregulated
M-CSF	129.83 ± 45.69	202.52 ± 134.26	<0.001	34.05 ± 10.96	0.004	Upregulated	Upregulated
SCGF-β	238762.25 ± 66376.59	243254.04 ± 109902.75	0.003	154560.48 ± 19826.99	0.08		Upregulated

Abbreviations: IL-2Rα, interleukin 2 receptor subunit alpha; IL, interleukin; RA, receptor antagonist; IFN, interferon; TNF-β, tumor necrosis factor beta; GM-CSF, granulocyte-macrophage colony-stimulating factor; p70, protein 70; MIG, monokine induced by gamma interferon; MIP, macrophage inflammatory protein; SDF, stromal cell-derived factor 1; MCP, monocyte chemotactic protein; LIF, leukemia inhibitory factor; MIF, macrophage migration inhibitory factor; RANTES, regulated upon activation normal T cell expressed and secreted; IP-10, interferon gamma-induced protein 10; TRAIL, tumor necrosis factor-related apoptosis inducing ligand; CTACK, cutaneous T-cell-attracting chemokine; bFGF, basic fibroblast growth factor; VEGF, vascular endothelial growth factor; NGF, nerve growth factor; PDGF-BB, platelet-derived growth factor-BB; G-CSF, granulocyte-colony stimulating factor; GRO, growth-regulated oncogene; HGF, human growth factor; SCF, stem cell factor; M-CSF, macrophage colony-stimulating factor; SCGF-β, stem cell growth factor beta; LECHV, Lechiguanas virus. *Insufficient data in control group prevented a calculated standard deviation. ^Significant upregulated in ANDV samples collected 5–10 days after symptom onset P=0.009).

Table S14. Random forest analysis of ANDV biomarkers and individual reproductive number (Z). Highest importance values signify a greater impact on model performance to predict Z. Negative importance values signify that removing it from the data will improve model performance.

Biomarker	Importance	P value
PDGF-BB	0.98	0.01
SCGF-β	0.58	0.03
TRAIL	0.42	0.04
GRO-α	0.36	0.03
IL-1β	0.23	0.05
IL-13	0.10	0.10
MCP-3	0.09	0.13
MIF	0.07	0.36
MIP-1β	0.07	0.26
SDF-1α	0.07	0.16
IL-10	0.06	0.21
LIF	0.05	0.38
β-NGF	0.05	0.29
IL-18	0.04	0.35
M-CSF	0.04	0.31
IP-10	0.03	0.48
G-CSF	0.03	0.44
TNF-β	0.02	0.40
IFN-α2	0.02	0.53
MIG	0.02	0.51
IL-4	0.02	0.52
IL-2Rα	0.01	0.47
IL-7	0.01	0.54
IL-17	0.01	0.54
IL-8	0.01	0.67
HGF	0.00	0.70
CTACK	-0.01	0.45
MIP-1α	-0.01	0.75
IL-16	-0.01	0.71
IL-1RA	-0.02	0.75
MCP-1	-0.02	0.75
TNF-α	-0.02	0.90
IL-9	-0.02	0.71
SCF	-0.02	0.60
Basic FGF	-0.03	0.83
Eotaxin	-0.03	0.53
IL-6	-0.03	0.87
RANTES	-0.06	0.90
IFN-γ	-0.09	0.95

Abbreviations: IL-2Rα, interleukin 2 receptor subunit alpha; IL, interleukin; RA, receptor antagonist; IFN, interferon; TNF-β, tumor necrosis factor beta; GM-CSF, granulocyte-macrophage colony-stimulating factor; p70, protein 70; MIG, monokine induced by gamma interferon; MIP, macrophage inflammatory protein; SDF, stromal cell-derived factor 1; MCP, monocyte chemotactic protein; LIF, leukemia inhibitory factor; MIF, macrophage migration inhibitory factor; RANTES, regulated upon activation normal T cell expressed and secreted; IP-10, interferon gamma-induced protein 10; TRAIL, tumor necrosis factor-related apoptosis inducing ligand; CTACK, cutaneous T-cell-attracting chemokine; bFGF, basic fibroblast growth factor; VEGF, vascular endothelial growth factor, NGF, nerve growth factor; PDGF-BB, platelet-derived growth factor-BB; G-CSF, granulocyte-colony stimulating factor; GRO, growth-regulated oncogene; HGF, human growth factor; SCF, stem cell factor; M-CSF, macrophage colony-stimulating factor; SCGF-β, stem cell growth factor beta.

Table S15. Orthohantavirus comparisons of gene pathway analysis using biomarker data trends

See attached excel file.

References

1. Castillo C, Naranjo J, Sepúlveda A, Ossa G, Levy H. Hantavirus pulmonary syndrome due to Andes virus in Temuco, Chile: clinical experience with 16 adults. Chest 2001;120:548-54.
2. Knust B, Macneil A, Rollin PE. Hantavirus pulmonary syndrome clinical findings: evaluating a surveillance case definition. Vector Borne Zoonotic Dis 2012;12:393-9.
3. Martinez VP, Bellomo CM, Cacace ML, Suárez P, Bogni L, Padula PJ. Hantavirus pulmonary syndrome in Argentina, 1995-2008. Emerg Infect Dis 2010;16:1853-60.
4. Alonso DO, Iglesias A, Coelho R, et al. Epidemiological description, case-fatality rate, and trends of Hantavirus Pulmonary Syndrome: 9 years of surveillance in Argentina. J Med Virol 2019;91:1173-81.
5. Bellomo CM, Pires-Marczeski FC, Padula PJ. Viral load of patients with hantavirus pulmonary syndrome in Argentina. J Med Virol 2015;87:1823-30.
6. Padula PJ, Edelstein A, Miguel SDL, López NM, Rossi CM, Rabinovich RD. Hantavirus pulmonary syndrome outbreak in Argentina: molecular evidence for person-to-person transmission of Andes virus. Virology 1998;241:323-30.
7. Bolger AM, Lohse M, Usadel B. Trimmomatic: a flexible trimmer for Illumina sequence data. Bioinformatics 2014;30:2114-20.
8. Martin M. Cutadapt removes adapter sequences from high-throughput sequencing reads. EMBnetjournal 2011;17.
9. Schmieder R, Edwards R. Quality control and preprocessing of metagenomic datasets. Bioinformatics 2011;27:863-4.
10. Langmead B, Salzberg SL. Fast gapped-read alignment with Bowtie 2. Nat Methods 2012;9:357-9.
11. Bankevich A, Nurk S, Antipov D, et al. SPAdes: a new genome assembly algorithm and its applications to single-cell sequencing. J Comput Biol 2012;19:455-77.
12. Meissner JD, Rowe JE, Borucki MK, St Jeor SC. Complete nucleotide sequence of a Chilean hantavirus. Virus Res 2002;89:131-43.
13. Li H, Handsaker B, Wysoker A, et al. The Sequence Alignment/Map format and SAMtools. Bioinformatics 2009;25:2078-9.
14. Ladner JT, Wiley MR, Mate S, et al. Evolution and spread of Ebola virus in Liberia, 2014-2015. Cell Host Microbe 2015;18:659-69.
15. Katoh K, Standley DM. MAFFT multiple sequence alignment software version 7: improvements in performance and usability. Mol Biol Evol 2013;30:772-80.
16. Kearse M, Moir R, Wilson A, et al. Geneious Basic: an integrated and extendable desktop software platform for the organization and analysis of sequence data. Bioinformatics 2012;28:1647-9.
17. Kugelman JR, Kugelman-Tonos J, Ladner JT, et al. Emergence of Ebola virus escape variants in infected nonhuman primates treated with the MB-003 antibody cocktail. Cell Rep 2015;12:2111-20.
18. Espy N, Pérez-Sautu U, Ramírez de Arellano E, et al. Ribavirin had demonstrable effects on the Crimean-Congo hemorrhagic fever virus (CCHFV) population and load in a patient with CCHF infection. J Infect Dis 2018;217:1952-6.
19. Guindon S, Dufayard J-F, Lefort V, Anisimova M, Hordijk W, Gascuel O. New algorithms and methods to estimate maximum-likelihood phylogenies: assessing the performance of PhyML 3.0. Syst Biol 2010;59:307-21.

20. Rambaut A. FigTree v1. 4. Molecular evolution, phylogenetics and epidemiology. Edinburgh, UK: University of Edinburgh, Institute of Evolutionary Biology; 2012.
21. Maleki KT, García M, Iglesias A, et al. Serum markers associated with severity and outcome of hantavirus pulmonary syndrome. J Infect Dis 2019;219:1832-40.
22. Wallinga J, Teunis P. Different epidemic curves for severe acute respiratory syndrome reveal similar impacts of control measures. Am J Epidemiol 2004;160:509-16.
23. Liaw A, Wiener M. Classification and regression by randomForest. *R* News 2002;2.3:18-22.
24. Altmann A, Toloşi L, Sander O, Lengauer T. Permutation importance: a corrected feature importance measure. Bioinformatics 2010;26:1340-7.
25. Wright MN, Ziegler A. ranger: A Fast Implementation of Random Forests for High Dimensional Data in C++ and R. arXiv 2018:1508.04409v2.
26. Cifuentes-Muñoz N, Salazar-Quiroz N, Tischler ND. Hantavirus Gn and Gc envelope glycoproteins: key structural units for virus cell entry and virus assembly. Viruses 2014;6:1801-22.
27. Jangra RK, Herbert AS, Li R, et al. Protocadherin-1 is essential for cell entry by New World hantaviruses. Nature 2018;563:559-63.
28. Jiang D-B, Sun L-J, Cheng L-F, et al. Recombinant DNA vaccine of hantavirus Gn and LAMP1 induced long-term immune protection in mice. Antiviral Res 2017;138:32-9.
29. Jiang D-B, Sun Y-J, Cheng L-F, et al. Construction and evaluation of DNA vaccine encoding hantavirus glycoprotein N-terminal fused with lysosome-associated membrane protein. Vaccine 2015;33:3367-76.
30. Levanov L, Iheozor-Ejiofor RP, Lundkvist Å, Vapalahti O, Plyusnin A. Defining of MAbs-neutralizing sites on the surface glycoproteins Gn and Gc of a hantavirus using vesicular stomatitis virus pseudotypes and site-directed mutagenesis. J Gen Virol 2019;100:145-55.
31. Geoghegan JL, Holmes EC. Predicting virus emergence amid evolutionary noise. Open Biol 2017;7:170189.
32. Park M, Loverdo C, Schreiber SJ, Lloyd-Smith JO. Multiple scales of selection influence the evolutionary emergence of novel pathogens. Philos Trans R Soc Lond B Biol Sci 2013;368:20120333.
33. Bartlett MS. The critical community size for measles in the United States. J R Stat Soc Ser A 1960;123:37-44.
34. Anderson RM, Anderson B, May RM. Infectious diseases of humans: dynamics and control. Oxford, UK: Oxford University Press; 1991.
35. Dalziel BD, Huang K, Geoghegan JL, et al. Contact heterogeneity, rather than transmission efficiency, limits the emergence and spread of canine influenza virus. PLoS Pathog 2014;10:e1004455.
36. Crawford PC, Dubovi EJ, Castleman WL, et al. Transmission of equine influenza virus to dogs. Science 2005;310:482-5.
37. Parrish CR, Holmes EC, Morens DM, et al. Cross-species virus transmission and the emergence of new epidemic diseases. Microbiol Mol Biol Rev 2008;72:457-70.
38. Khaiboullina SF, Levis S, Morzunov SP, et al. Serum cytokine profiles differentiating hemorrhagic fever with renal syndrome and hantavirus pulmonary syndrome. Front Immunol 2017;8:567.